The effect of anthropogenic emission, meteorological factors, and carbon dioxide on the surface ozone increase in China from 2008 to 2018 during the East Asia summer monsoon season

Danyang Ma[1], Tijian Wang[1,*], Hao Wu[2], Yawei Qu[3], Jian Liu[4], Jane Liu[5], Shu Li[1], Bingliang Zhuang[1], Mengmeng Li[1], Min Xie[1]

[1]School of Atmospheric Sciences, Nanjing University, Nanjing 210023, China.

[2]Key Laboratory of Transportation Meteorology of China Meteorological Administration, Nanjing Joint Institute for Atmospheric Sciences, Nanjing 210000, China.

[3]College of Intelligent Science and Control Engineering, Jinling Institute of Technology, Nanjing 211169, China.

[4]Key Laboratory for Virtual Geographic Environment of Ministry of Education；Jiangsu Center for Collaborative Innovation in Geographical Information Resource Development and Application；School of Geography Science, Nanjing Normal University, Nanjing, China 210023.

[5]Department of Geography and Planning, University of Toronto, Toronto M5S 2E8, Canada.

Correspondence to: Tijian Wang (tjwang@nju.edu.cn)

Abstract. Despite the implementation of the Clean Air Action Plan by the Chinese government in 2013, the issue of increasing surface ozone (O_3) concentrations remains a significant environmental concern in China. In this study, we used an improved regional climate-chemistry-ecology model (RegCM-Chem-YIBs) to investigate the impact of anthropogenic emissions, meteorological factors, and CO_2 changes on summer surface O_3 levels in China from 2008 to 2018. Compared to its predecessor, the model has been enhanced concerning the photolysis of O_3 and the radiative impacts of CO_2 and O_3. The investigations showed anthropogenic emissions were the primary contributor to the O_3 increase in China, responsible for 4.08~18.51 ppb in the North China Plain. However, changed meteorological conditions played a crucial role in decreasing O_3 in China and may have a more significant impact than anthropogenic emissions in some regions. ~~In Pearl River Delta, for example, the contributions of meteorological conditions and anthropogenic emissions on O_3 were -1.29 and 0.81 ppb in 2013, respectively. CO_2 was critical in O_3 variations, especially in southern China,~~Changed CO_2 played a critical role in the variability of O_3 through radiative forcing and isoprene emissions, particularly in southern China, inducing an increase in O_3 on the southeast coast of China (0.28~0.46 ppb~~ a^{-1}~~) and a decrease in the southwest and central China (-0.51~-0.11 ppb~~ a^{-1}~~). Our study comprehensively analyzed O_3 variation across China from various perspectives and highlighted the importance of considering CO_2 variations when designing long-term O_3 control policies, especially in high vegetation coverage areas.

1 Introduction

O_3 is a strong oxidant detrimental to human health (Lu et al., 2020; Liu et al., 2018a) and vegetation growth~~the ecosystem~~ (Monks et al., 2015; Wang et al., 2017a). Furthermore, it is a crucial active compound influencing the earth's radiative balance~~specie of radiation~~, with an effective radiative forcing of up to 0.47 W/m^2 in 2019 (Ipcc, 2021). Tropospheric O_3 has garnered significant attention over the past few decades due to its crucial role in air quality and climate change (Duan et al., 2017; Li et al., 2019; Ashmore and Bell, 1991; Lu et al., 2018).

With the rapid development in China, emissions of O_3 precursors have been on the rise, leading to an annual increase in O_3 concentrations since the beginning of the 20th century (Liu and Wang, 2020a; Ma et al., 2016). Surface O_3 pollution has become a severe air quality concern in China (Verstraeten et al., 2016; Xu et al., 2018), particularly in major urban areas such as the North China Plain (NCP), Fenwei Plain (FWP), Yangtze River Delta (YRD), Pearl River Delta (PRD), and the Sichuan Basin (SCB) (Wang et al., 2020; Wang et al., 2017a; Yin and Ma, 2020; Shen et al., 2019; Zhao et al., 2018; Wang et al., 2009). Although the Chinese government initialized~~performed~~ the Clean Air Action Plan in 2013 to control air pollution, the concentration of O_3 precursors and $PM_{2.5}$ has significantly decreased (Zhai et al., 2019). However, surface O_3 concentrations continue to increase in major urban areas.

Recent studies have suggested that regional meteorological conditions influence surface O_3 levels through various pathways (Jacob and Winner, 2009; Shen et al., 2016; Lin et al., 2008). Modeling studies have shown that O_3 levels are sensitive to temperature, humidity, wind speed, mixing height, and other meteorological conditions (Pfister et al., 2014; Sanchez-Ccoyllo et al., 2006). For instance, temperature affects the chemical formation rate of O_3 (Lee et al., 2014), while precipitation reduces surface O_3 concentrations through wet removal (Fang et al., 2011). Additionally, the elevated planetary boundary layer (PBL) height enhances upward movement,

resulting in lower surface O_3 concentrations (Haman et al., 2014). Therefore, long-term modeling of surface O_3 levels must consider changes in meteorological conditions.

CO_2 is the primary anthropogenic radiative force of the climate system (Gauss et al., 2003; Schimel et al., 2015). CO_2 can impact regional air temperature and precipitation, leading to changes in surface O_3 concentrations (Lu et al., 2013; Yang et al., 2014).

On the other hand, Biogenic volatile organic compounds (BVOCs) are significant O_3 precursors, and isoprene is the primary specie among BVOCs that vegetation emits (Zheng et al., 2009; Fiore et al., 2011). In most of China, O_3 is volatile organic compounds (VOCs)-limited in the summer, especially in industrial cities (Li et al., 2018; Wu et al., 2018). Thus, it plays a significant role in modulating O_3 levels and positively correlates with O_3 concentrations in major urban areas of China. It is known that CO_2 can enhance vegetation's photosynthesis (Sun et al., 2013; Heald et al., 2009; Tai et al., 2013; Monson and Fall, 1989), which may directly increase isoprene emission (Rapparini et al., 2004). Based on the observation, Rosenstiel et al. (2003) found that the isoprene emissions of plants grew by about 21% and 41% when CO_2 reached 800 ppm and 1200 ppm, respectively. However, Wilkinson et al. (2009) indicated that different vegetation types show varying responses in isoprene emission when CO_2 increases. Isoprene emission was decreased by 30~40% in Populus tremuloides Michx but increased by about 100% in Quercus rubra when CO_2 concentrations were grown (Sharkey et al., 1991). High concentrations of CO_2 may inhibit the emission of isoprene by reducing the activity of BVOCs synthetase or decreasing the synthesis of adenosine triphosphate (Possell et al., 2005). Guenther et al. (1991) also indicated that isoprene emissions were significantly reduced when CO_2 was increased from 100 to 600 μmol mol^{-1}. In summary, the impact of elevated CO_2 on isoprene emission may be positive or negative, mainly related to the relative size of the inhibition caused by elevated CO_2 and promotion by enhanced photosynthesis.

Numerous studies have concluded that anthropogenic emissions are the primary drivers of surface O_3 increases in different regions or years in China. Meanwhile, the effects of meteorological parameters can be substantial~~should not be negligible~~ (Wang et al., 2019c; Lu et al., 2019; Dang et al., 2021; Liu and Wang, 2020a). For instance, Li et al. (2020) indicated that anthropogenic emissions were the primary cause of surface O_3 increase in China from 2013 to 2019. Liu and Wang (2020a) suggested that anthropogenic emissions play a dominant role in the O_3 variety in China, but the effects of meteorological conditions could be more significant in some regions. Han et al. (2020) analyzed the O_3 changes in summer and suggested that meteorology can explain about 43% of that in eastern China.

Previous studies have mainly focused on the impact of anthropogenic emissions and meteorological factors on the rise of O_3 levels, with limited attention given to the role of CO_2 variations. However, due to the rapid socioeconomic growth in China and the subsequent surge in energy consumption, CO_2 emissions, and concentrations have also increased significantly, particularly in the eastern coastal region~~Most previous research focused on the effects of anthropogenic emission and meteorological factors on O_3 increase, ignoring the contributions of CO_2 variations. And CO_2 emission has kept annual increasing in China~~ (Lv et al., 2020; Ren et al., 2014). Furthermore, given the significant impact of CO_2 on O_3, it is crucial to evaluate the influence of changes in CO_2 concentration on the maximum daily 8-hour average (MDA8) O_3 concentrations at the surface. Thus, a comprehensive assessment of the impact of anthropogenic emissions, meteorological factors, and CO_2 on surface O_3 is imperative.~~Therefore, a~~

~~comprehensive evaluation of the impact of anthropogenic emission, meteorological factors, and carbon dioxide on surface maximum daily 8 h average (MDA8) O_3 is necessary~~

Here, we employed an advanced regional climate-chemistry-ecology model to assess the impact of anthropogenic emissions, meteorological factors, and carbon dioxide variations during the summer monsoon period (May, June, July, and August) on surface O_3 levels. Our findings can facilitate the development of a comprehensive O_3 improvement strategy. Sect. 2 describes the methods and data, and the results and discussion are given in Sect. 3, finally, the conclusions are shown in Sect. 4.

2 Methods and data

2.1 Measurement data

We compared the simulated regional meteorological factors with the European Centre for Medium-Range Weather Forecasts Interim reanalysis data (ERA-Interim) at 37 vertical levels, which included temperature, relative humidity, and wind speed (Balsamo et al., 2015; Hoffmann et al., 2019). The observed surface O_3 was taken from the China National Environmental Monitoring Center (CNEMC), which had more than 1400 environmental monitoring stations in 2018 (Wang et al., 2018; Kong et al., 2021; Zheng et al., 2014). The World Data Centre for Greenhouse Gases (WDCGG) data (Liu et al., 2009; Li et al., 2017) was applied to evaluate the simulated surface CO_2 concentrations. The monitoring stations of O_3 and CO_2 are shown in Figure. 1.

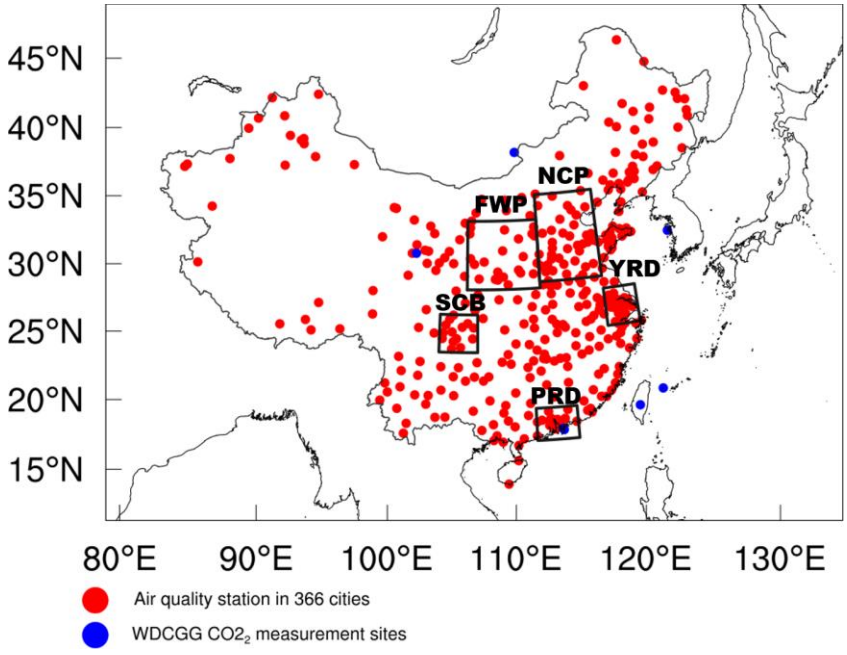

Figure 1. Model domains for the RegCM-Chem-YIBs model. The regions with black boundaries are the North China Plain (34~41°N, 113~119°E), the Yangtze River Delta (30~33°N, 119~122°E), the Pearl River Delta (21.5~24°N, 112~115.5°E), the Sichuan Basin (28.5~31.5°N, 103.5~107°E), and the Fenwei Plain (33.5~39°N, 106~113°E) regions.

.

2.2 Model description

~~The RegCM-Chem-YIBs is a regional climate-chemistry-ecology model developed by a team of Prof. Wang in the School of Atmospheric Sciences of Nanjing University (Xie et al., 2020; Xie et al., 2019), the International Center for Theoretical Physics (ICTP) in Italy (Giorgi et al., 2012; Giorgi and Mearns, 1999), and a team led by Prof. Yue in Nanjing University of Information Technology (Yue and Unger, 2015).~~ The RegCM-Chem-YIBs is a regional climate-chemistry-ecology model developed from the RegCM model RegCM is a regional climate model initially developed by the International Center for Theoretical Physics (ICTP) (Giorgi et al., 2012). Shalaby et al. (2012) integrated the Chem chemistry model into the RegCM model and incorporated the condensed version of the Carbon Bond Mechanism (CBM-Z) to enhance the model's capabilities. To further improve the model's performance, Yin et al. (2015) added a Volatility Basis Set (VBS) scheme to simulate Secondary Organic Aerosols (SOA). Xie et al. (2020) further modified the model by incorporating CO_2 as a tracer, which is subject to regulation by sources, sinks, and atmospheric transport processes. The model represents the four sources and sinks of CO_2 as surface fluxes, including emissions from fossil fuels and biomass burning, air-sea CO_2 exchange, and terrestrial biosphere CO_2 fluxes. Additionally, the model incorporated the Yale Interactive Terrestrial Biosphere (YIBs), a land carbon cycle model that enables the simulation of ecological processes, including carbon assimilation, allocation, and autotrophic and heterotrophic respiration (Yue and Unger, 2015).

The ecological model (YIBs) was fully coupled into the regional climate-chemical model (RegCM-Chem) to reproduce the interactions between atmospheric composition and the ecosystem in the ~~authentic~~ actual atmosphere (Xie et al., 2019). The meteorological factors and air components simulated by RegCM-Chem were input into the YIBs model to simulate vegetation physiological processes and calculate land surface parameters such as carbon dioxide flux, ~~Biogenic volatile organic compound (~~BVOCs~~)~~ emissions, and stomatal conductance. Conversely, the simulations of the YIBs model were fed back into the RegCM-Chem model to adjust the air qualities, temperature, humidity, circulation, and other meteorological fields. The RegCM-Chem-YIBs has been extensively applied to study surface O_3, $PM_{2.5}$, CO_2, the summer monsoon, and the interactions between air quality and the ecosystem (Zhuang et al., 2018; Pu et al., 2017; Xu et al., 2022a; Xie et al., 2018; Ma et al., 2023).

The RegCM model offers a variety of physical and chemical parameterization options. Here, the climatological chemical boundary conditions were driven by the Model of Ozone and Related Chemical Tracers (MOZART). The gas-phase chemistry employed the CBM-Z scheme (Zaveri and Peters, 1999). For the boundary layer scheme, the Holtslag PBL approach was utilized (Khayatianyazdi et al., 2021). The Grell cumulus convection scheme was employed to simulate convective processes (Grell, 1993). The CCM3 radiation scheme and CLM3.5 land surface module were used in the model (Collins et al., 2006; Giorgi and Mearns, 1999; Decker and Zeng, 2009).

2.3 Model improvements

~~The previous version RegCM-Chem-YIBs model simulated the radiation effect that considers spatial-temporal variations of PM only. The air CO_2 and O_3 concentrations in the radiation module were constant in the year to calculate the radiation. We have taken simulated CO_2 and O_3 concentrations with a spatiotemporal variation into the radiation module and improved the associated radiation effects to better simulate the regional radiation balance.~~

~~Lefer et al. (2003) suggested that better aerosol optical parameter inputs, including aerosol optical depth (AOD) and single scattering albedo (SSA), played a significant role in the photolysis of O_3. We improved the calculation involving the AOD and SSA in the photolysis subroutine so that the extinction effect of the particles can be fed back to the photolysis reaction correctly. These improvements led to more realistic simulations in air components and regional meteorology.~~

2.3.1 Radiation

In the previous version of the RegCM-Chem-YIBs model, radiative calculations only accounted for changes in the spatiotemporal distribution of particulate matter. To simplify the radiation calculations, the atmospheric CO_2 and O_3 concentrations were assumed to be constant throughout the year. However, atmospheric CO_2 and O_3 are subject to modulation by various sources, sinks, physical processes, and chemical processes (Ballantyne et al., 2012; Wang et al., 2019a). Additionally, rapid urbanization in China has led to an annual increase in CO_2 and O_3 concentrations (Guan et al., 2021; Wei et al., 2022), with elevated concentrations and growth rates primarily distributed in the eastern regions where urbanization is most prominent (Shi et al., 2016; Wang et al., 2017b). To more accurately simulate the atmospheric radiation balance and East Asian monsoon climate, it is necessary to incorporate spatiotemporal variations of CO_2 and O_3 concentrations into the radiation module. Therefore, we included the varying CO_2 and O_3 concentrations simulated by the model in the radiation module to calculate the corresponding radiative forcing.

2.3.2 Photolysis

The photolysis process was simulated using the Tropospheric Ultraviolet and Visible (TUV) model, which is commonly used to compute photolysis rates in various models (Tie et al., 2003; Shetter et al., 2002; Borg et al., 2011). The TUV model employs input parameters such as zenith angle, altitude, ozone column, SO_2 column, NO_2 column, aerosol optical depth (AOD), single scattering albedo (SSA), and albedo, among others, to calculate photolysis rates (Singh and Singh, 2004). However, in the TUV module of the RegCM-Chem-YIBs model, AOD and SSA were held constant. This is problematic as accurate aerosol optical parameters, such as AOD and SSA, play a crucial role in the photolysis of O_3 (Lefer et al., 2003). To address this issue, we incorporated temporally and spatially varying AOD and SSA simulated by the RegCM-Chem-YIBs model into the photolysis rate calculations in the TUV module. This enabled us to accurately incorporate the extinction effect of the varying particles into the photolysis reaction, leading to more realistic simulations of air components and regional meteorology.

2.4 Emissions and Experiment settings

Anthropogenic emissions from 2008 to 2018 were obtained from the Multi-resolution Emission Inventory for China (MEIC), which has been compiled and maintained by Tsinghua University since 2010 (Zheng et al., 2018; Wang et al., 2014). CO_2 emissions and boundary conditions were derived from the NOAA CarbonTracker CT2019 dataset (Jacobs et al., 2021). The initial meteorological boundary data, such as temperature, relative humidity, and wind, are derived from the ERA-Interim reanalysis dataset with a horizontal resolution of 0.125°, a temporal resolution of 6 hours, and 37 vertical levels (Liu et al., 2018b). The weekly mean Sea Surface Temperature dataset was obtained from the National Ocean and Atmosphere Administration (NOAA) (Reynolds et al., 2002).

~~The Model of Ozone and Related Chemical Tracers (MOZART) model was chosen to drive climatological chemical boundary conditions. (Zaveri and Peters, 1999) The boundary layer scheme was Holtslag PBL (Khayatianyazdi et al., 2021). The Grell cumulus convection scheme was employed (Grell, 1993). The CCM3 radiation scheme and CLM3.5 land surface module were used in the model (Collins et al., 2006; Giorgi and Mearns, 1999; Decker and Zeng, 2009).~~

The simulation domain was illustrated in Figure 1, with the target region centered at 36°N and 107°E, and a grid resolution of 60 km by 60 km. The model used 18 vertical levels, ranging from the surface to 50 hPa.

~~The interannual changing anthropogenic emissions, meteorological fields, and CO_2 emissions were applied in the base experiment during the summer monsoon period from 2008 to 2018. The meteorological conditions were maintained at 2008 in all ten years, namely the $SIM_{i,m=2008}$ experiment.~~

~~The changes in O_3 concentrations from 2009 to 2018 relative to 2008 were obtained by comparing the simulations of different years with 2008 in the base experiment (Eq. (1)). The effect of meteorology in the O_3 was obtained by comparing the results between $SIM_{i,m}$=2008 with the base experiment in the same year (Eq. (2)). Similarly, the effects of CO_2 emissions were derived (Eq. (3)). Finally, the influence of anthropogenic emissions was calculated by excluding the impact of meteorological factors and CO_2 from the changes in O_3 concentrations (Eq. (4)). The numerical experiments are shown in table 1.~~In the Base experiment, we incorporated interannual variations in anthropogenic emissions, meteorological fields, and CO_2 emissions. Meteorological conditions (CO_2 emissions) were kept constant at 2008 levels over ten years, referred to as the $SIM_{MET=2008}$ ($SIM_{CO2=2008}$) experiment.

The changes in O_3 concentrations relative to 2008 between 2009 and 2018 were determined by comparing simulations of different years with 2008 in the Base experiment (Eq. (1)). The impact of changed meteorological conditions on O_3 concentrations relative to 2008 was assessed by comparing results between $SIM_{MET=2008}$ and the Base experiment in the same year (Eq. (2)). The contribution of changed CO_2 emissions was similarly estimated (Eq. (3)). Finally, the influence of anthropogenic emissions was calculated by excluding the impact of meteorological factors and CO_2 from the changes in O_3 concentrations (Eq. (4)). Table 1 shows the results of the numerical experiments.

$$\Delta O_i = Base_i - Base_{2008} \quad (1)$$

$$\Delta M_i = Base_i - SIM_{i,MET=2008} \quad (2)$$

$$\Delta C_i = Base_i - SIM_{i,CO2=2008} \quad (3)$$

$$\Delta E_i = \Delta O_i - \Delta M_i - \Delta C_i \quad (4)$$

ΔO_i : The changes in O_3 concentrations in the year i relative to 2008.
$Base_i$: The O_3 concentrations in the Base experiment in the year i.
ΔM_i : The changes in O_3 concentrations in the year i due to meteorological factors variations.
$SIM_{i,MET=2008}$: The O_3 concentrations in the $SIM_{MET=2008}$ experiment in the year i.
ΔC_i : The changes in O_3 concentrations in the year i due to CO_2 variations.
$SIM_{i,CO2=2008}$: The O_3 concentrations in the $SIM_{CO2=2008}$ experiment in the year i.

ΔE_i : The changes in O_3 concentrations in the year i due to anthropogenic emissions variations.

Table 1. The Numerical experimental in this study.

~~Experiment~~	~~Time~~	~~Description~~
~~Base~~	~~2008-2018~~	~~Interannual changing anthropogenic emissions, meteorological fields, and CO_2 emissions~~
~~SIM_MET08~~	~~2009-2018~~	~~Meteorological conditions remained at 2008~~
~~SIM_$CO_2$08~~		~~CO_2 emissions remained at 2008~~

Experiment	Time	Meteorological fields	CO_2 emissions	Anthropogenic emissions
Base	2008-2018	Varying	Varying	Varying
$SIM_{MET=2008}$	2009-2018	2008	Varying	Varying
$SIM_{CO2=2008}$		Varying	2008	Varying

In this work, both meteorological and CO_2 boundary conditions were kept consistent in base and sensitivity studies. We did not consider the impact of boundary conditions on O_3 due to the following reasons. First, in general, the regional model was coupled with the global model to get a more realistic influence from the boundary. However, for long-term climate-chemistry modeling, the such coupling means a large computing resource. Second, the boundary conditions were derived from global models (Liu et al., 2017; Ban et al., 2014) and have to be prescribed in sensitive experiments. Finally, fixed boundary conditions were widely used in some O_3 studies in China (Liu and Wang, 2020a, b; Wang et al., 2019b). Moreover, regional emissions are the primary source of surface O_3 in China, with contributions accounting for 80% from May to August (Lu et al., 2019). Therefore, the impact of fixed boundary conditions can be ignored in the current stage.

3 Results and discussion

3.1 Model evaluation

The ability of RegCM to reproduce East Asian climate and air quality has been widely evaluated in recent years. Previous studies have demonstrated that RegCM was capable of the essential characteristics and interannual variations of air components and meteorological fields in East Asia (Xu et al., 2022b; Ma et al., 2023; Zhuang et al., 2018). Given that the monitoring of near-surface O_3 levels by CNEMC was initiated only in late 2013, the monitoring sites in 2013 and 2014 were limited, and the monitoring period was disjointed. As a result, in this study, we compared the simulated meteorological fields, O_3, and CO_2 levels with observations only from 2015 to 2018.~~Here, for more confidence, the meteorological fields, O_3 and CO_2 are compared between simulations and observations in 2018.~~

Figures S1~4 demonstrated that the RegCM-Chem-YIBs model effectively captured the spatial distribution and magnitude of temperature, humidity, and wind over East Asia at 500 hPa, 850 hPa, and 1000 hPa between 2015 and 2018. However, due to the complex terrain's influence on the lower atmosphere, most models show better results at higher levels (Zhuang et al., 2018; Anwar et al., 2019; Xie et al., 2019). Thus, the simulations at 500 hPa were more consistent with the reanalysis data. At 1000 hPa, the simulated wind speed was slightly higher than the reanalysis data in eastern China. This difference may be due to common deficiencies in meteorological models, such as insufficient horizontal resolution, initial and boundary conditions, and physical parameterizations (Cassola and Burlando, 2012; Accadia et al., 2007), particularly in areas with low wind speeds (Carvalho et al., 2012).

~~Figure 2 shows the RegCM-Chem-YIBs model has well captured the spatial distribution and magnitude of temperature, humidity, and wind over East Asia at 850 hPa and 200 hPa. The model underestimated the temperatures and wind speed slightly at 850 hPa. In contrast, the relative humidity was overpredicted by about 10% at 850 hPa. Due to the influences of complex terrain on the lower atmosphere, most models show better results at higher levels (Zhuang et al., 2018; Anwar et al., 2019; Xie et al., 2019). Therefore, the simulations at 200 hPa are closer to the reanalysis data.~~

~~The evaluations of surface O_3 and CO_2 in East Asia are shown in Table 2.~~ Figures S5 and S6 demonstrated that the model accurately reproduced the observed increase in surface CO_2 and O_3 from 2015 to 2018, with high correlation coefficients ranging from 0.39 to 0.74 (Table 2). The model effectively captured the high concentrations of O_3 in major urban areas such as the NCP, the YRD, the PRD, the SCB, and the FWP, while also successfully reproducing the gradient in CO_2 concentrations between eastern and western China. However, the model slightly underpredicted MDA8 O_3 concentrations (-4.02 to -3.21 ppb) and overestimated CO_2 levels (3.32~7.07 ppm). These discrepancies are mainly attributed to uncertainties in the emissions inventory (Hong et al., 2017). Overall, the simulated meteorological factors and surface CO_2 and O_3 concentrations were deemed acceptable.

~~The RegCM-Chem-YIBs model reality reproduced surface O_3 and CO_2 concentrations during the East Asia summer monsoon season, with high correlation coefficients (0.73 for O_3 and 0.41 for CO_2). The overpredicted MDA8 O_3 (1.73%) and CO_2 (6.57%) were mainly driven by the uncertainty of the emissions inventory (Wang et al., 2014; Hong et al., 2017; Zhang et al., 2014). The normalized mean bias was 6.63% and 1.73%, respectively. Therefore, the simulated meteorological factors and surface O_3 and CO_2 were acceptable.~~

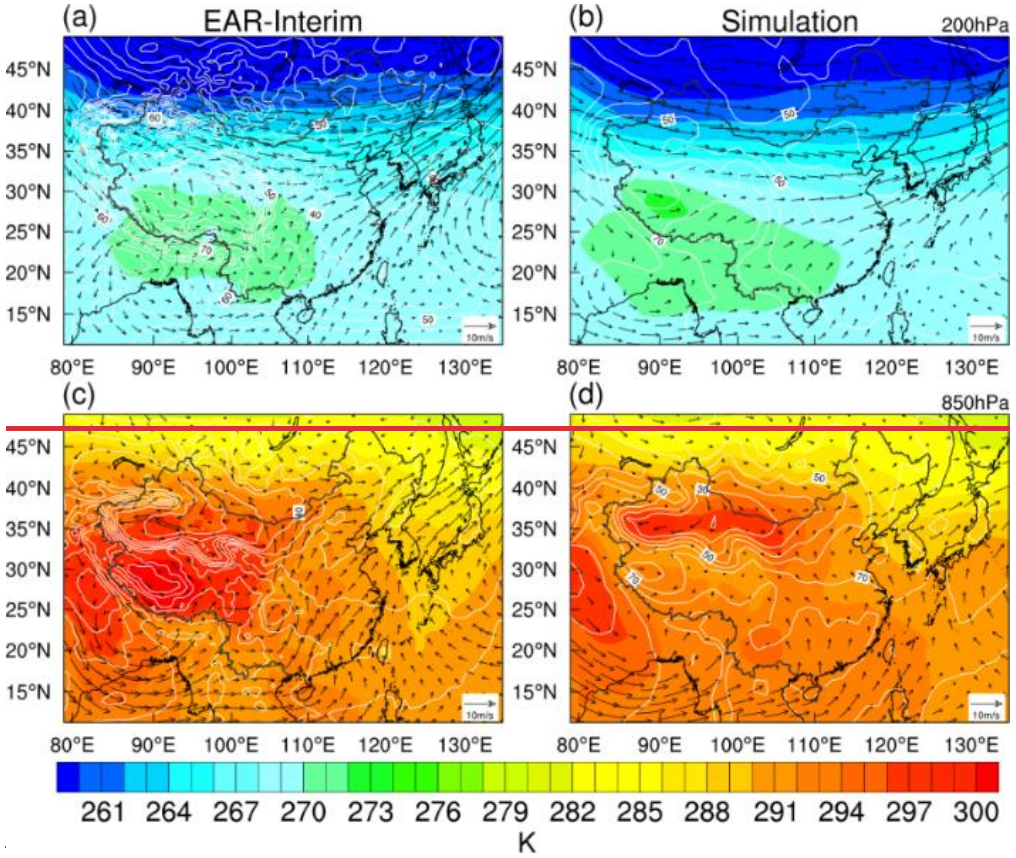

~~**Figure 2.** Comparisons between the simulated (a, c) and reanalysis (b, d) mean temperature (shading, units: K), wind (vectors, units: m/s), and relative humidity (contours, units: %) at 200 hPa (a, b) and 850 hPa (c, d).~~

Table 2. Evaluations of the surface CO_2 (units: ppm) and MDA8 O_3 (units: ppb) during the summer monsoon period in East Asia.

~~Species~~	~~OBS~~	~~SIM~~	~~MB~~	~~NMB（%）~~	~~RMSE~~	~~R~~
~~CO_2（ppm）~~	~~409.61~~	~~416.68~~	~~7.07~~	~~1.73~~	~~11.32~~	~~0.41~~
~~MDA8O_3（ppb）~~	~~52.08~~	~~55.53~~	~~3.42~~	~~6.63~~	~~24.78~~	~~0.73~~
Species	Year	OBS	SIM	MB	RMSE	R
CO_2（ppm）	2015	402.82	406.98	4.16	9.37	0.44
	2016	407.12	410.44	3.32	8.22	0.69
	2017	408.35	413.62	5.27	11	0.39
	2018	409.61	416.68	7.07	11.32	0.41
MDA8 O_3（ppb）	2015	48.77	44.75	-4.02	29.39	0.57
	2016	50.16	46.95	-3.21	27.56	0.60
	2017	55.43	51.87	-3.56	21.55	0.74
	2018	55.53	52.08	-3.42	24.78	0.73

OBS: observation; SIM: simulation; MB: bias; NMB: normalized mean bias; RMSE: root mean square error; R: correlation coefficient. MDA8 O_3: the maximum daily 8-hour average O_3.

3.2 Ozone variation from 2008 to 2018

Figure S7~~3~~ illustrates the mean seasonal MDA8 O_3 concentrations in East Asia during the summer monsoon period from 2008 to 2018. High O_3 concentrations appeared in eastern China, which can be attributed to increased emissions, high temperatures, humidities, and intense radiation in the region (Gao et al., 2020; Mousavinezhad et al., 2021; Wei et al., 2022). Surface O_3 increased annually in most of China between 2008 to 2018, with megacity clusters experiencing a more significant increase.

We conducted a regional analysis of surface O_3 increases in five target regions: the NCP, the YRD, the PRD, the SCB, and the FWP. In 2018, the surface MDA8 O_3 concentrations averaged 74 ppb in the NCP region, while the other areas had lower concentrations (ranging from 42 to 67 ppb in the FWP, YRD, PRD, and SCB). The lower surface O_3 levels in the SCB and FWP regions were attributed to lower anthropogenic emissions. The YRD and PRD regions were more affected by meteorological factors, with the East Asian summer monsoon bringing in cleaner air and precipitation from the sea, leading to lower air pollution concentrations (He et al., 2012). The spatial distribution and increasing trend of surface MDA8 O_3 concentrations in China were consistent with previous studies (Li et al., 2020; Shen et al., 2022).

Figure 2~~4~~ and Table 3 illustrate the changes in surface MDA8 O_3 concentrations from 2009 to 2018 relative to 2008. The surface MDA8 O_3 concentrations in China increased drastically over the past decade, particularly in 2017 and 2018 (6.79~32.03 ppb). We divided the period from 2009 to 2018 into two phases based on the Clean Air Action Plan implemented in 2013: the pre-governance period (PreG, 2009~2013) and the post-governance period (PostG, 2014~2018). ~~Table 5 shows t~~The surface MDA8 O_3 concentration increased significantly in NCP (18.42 ppb~~ a^{-1}~~), followed by SCB (11.21 ppb~~ a^{-1}~~), FWP (10.9 ppb~~ a^{-1}~~), and the YRD (10.07 ppb~~ a^{-1}~~), while increased slightly in PRD (4.94 ppb~~ a^{-1}~~), in PosG relative to 2008. Our results were consistent with previous studies by Lu et al. (2020), Ma et al. (2016), and Mousavinezhad et al. (2021).

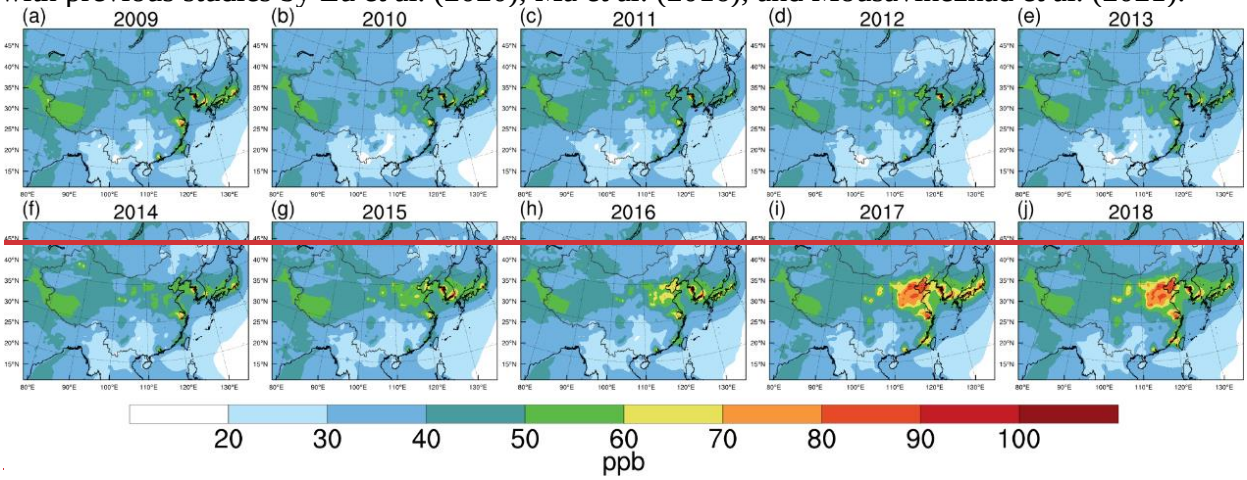

~~**Figure 3.** Simulated surface MDA8 O_3 concentrations in the summer monsoon period of 2009 (a), 2010 (b), 2011 (c), 2012 (d), 2013 (e), 2014 (f), 2015 (g), 2016 (h), 2017 (i) and 2018 (j).~~

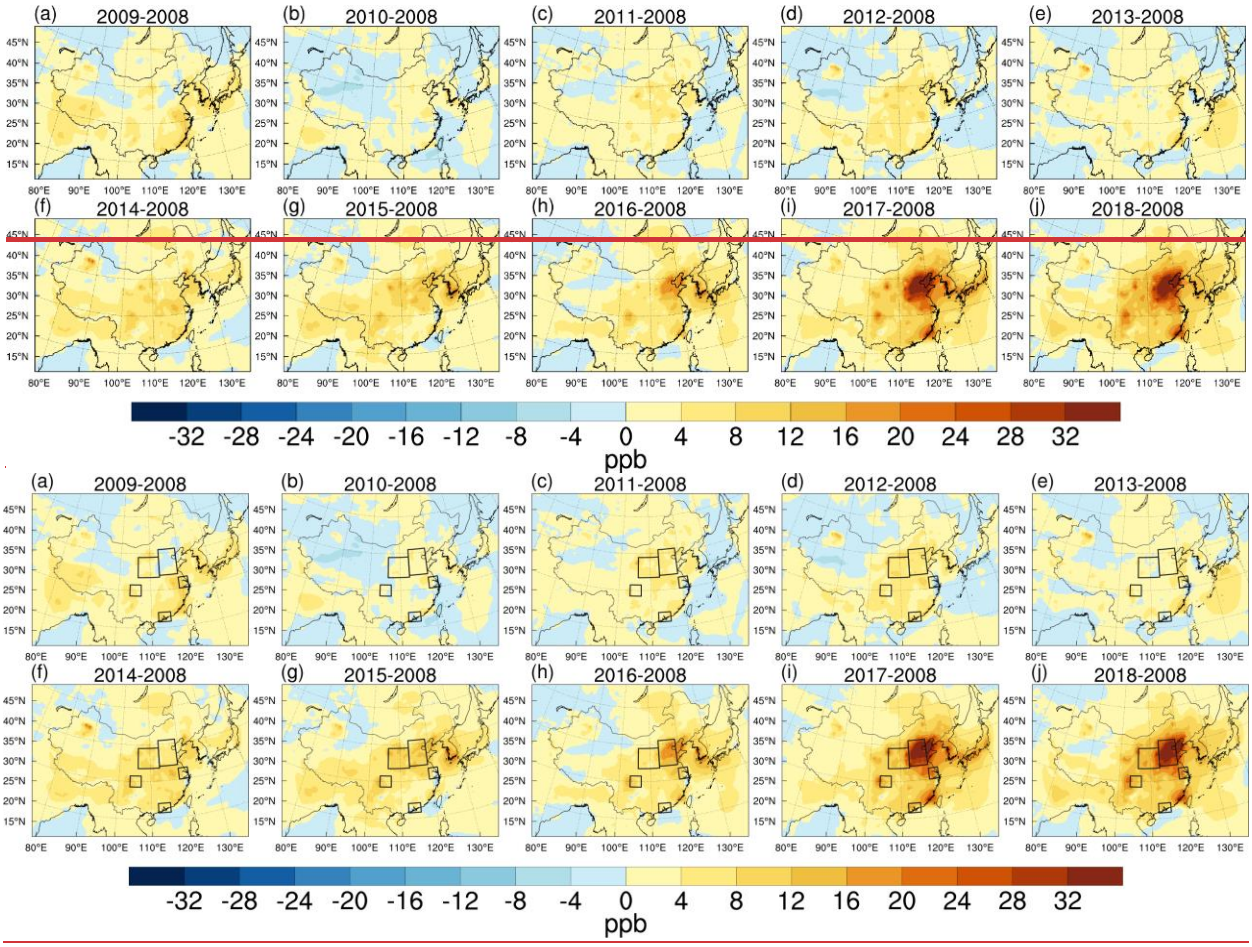

Figure 24. Changes in the surface MDA8 O_3 concentrations (units: ppb) during the summer monsoon period from 2009 (a), 2010 (b), 2011 (c), 2012 (d), 2013 (e), 2014 (f), 2015 (g), 2016 (h), 2017 (i) and 2018 (j) relative to 2008.

Table 3. The changes of MDA8 O_3 over North China Plain, Fenwei Plain, Yangtze River Delta, Pearl River Delta, and Sichuan Basin during the summer monsoon period from 2009 to 2018 relative to 2008.

Regions	2009	2010	2011	2012	2013	2014	2015	2016	2017	2018	PreG	PostG
NCP	0.14	2.85	4.53	6.13	2.7	4.78	10.1	14.25	30.92	32.03	3.27	18.42
FWP	3.23	1.78	5.01	6.78	1.37	7.9	10.5	6.24	13.71	16.17	3.63	10.90
YRD	8.33	1.47	1.46	0.5	3.12	6.04	3.46	7.09	17.64	16.12	2.98	10.07
PRD	5.76	-0.26	2.56	5.13	-0.4	3.82	1.46	3.16	9.45	6.79	2.56	4.94
SCB	4.92	1.03	3.46	5	3.94	8.54	9.27	9.78	13.67	14.8	3.67	11.21

3.3 The effect of meteorology in 2008~2018 ozone increase

Overall, the meteorological variations from 2008 to 2018 were unfavorable for O_3 increase during the EASM period, as illustrated in Figure 3~~The meteorological factors were generally unfavorable to O_3 formation during the study period (Fig. 5)~~.

Based on Figure 3 and Table 4, it is evident that meteorological conditions had a significant impact on surface MDA8 O_3 in the NCP and FWP regions during the PostG period (-0.09~-0.04 ppb~~a^{-1}~~) compared to the PreG period (-1.41~-0.88 ppb~~a^{-1}~~). In the SCB region, the impact of

meteorological fields was relatively weak (-0.41~0.71 ppb ~~a^{-1}~~), attributed to the basin topography and stable atmospheric conditions. However, in the eastern and southeastern coastal areas of China, due to the significant influence of the EASM, the impact of meteorological conditions may be more critical than that of anthropogenic emissions. For instance, in the YRD and PRD regions, meteorological conditions significantly changed O_3 levels (-1.29~1.3 ppb ~~a^{-1}~~) compared to anthropogenic emissions (0.81~0.87 ppb ~~a^{-1}~~) in 2013, indicating the significant influence of meteorological conditions on surface O_3.

Our findings are consistent with previous studies. Liu and Wang (2020a) reported a decrease in O_3 in Shanghai from 2013 to 2017 due to changes in meteorological conditions. Chen et al. (2019) and Liu and Wang (2020a) also suggested that altered meteorological conditions had a negative impact on O_3 formation in the NCP and FWP regions, and that the influence of meteorology on surface-level O_3 decreased in PostG.~~indicated meteorology factors are unfavorable to O_3 formation in NCP and FWP, and the influence of meteorology on surface O_3 decreased in PostG.~~ In addition, Cheng et al. (2019) found that the effects of meteorological conditions on long-term O_3 variations were less than 3%, which is similar to our study.

As we know, the formation of surface O_3 is promoted by rising temperatures (Steiner et al., 2010). However, increased surface temperatures can also intensify turbulence within the planetary boundary layer (PBL), increasing PBL height (Guo et al., 2016). This increase in PBL height, coupled with the enhanced upward motion, can transport near-surface pollutants to the upper atmosphere, reducing their concentration in the lower atmosphere (Gao et al., 2016). Additionally, the upward motion can also facilitate cloud formation and precipitation, resulting in a reduction of near-surface atmospheric pollutants via precipitation washout (Yoo et al., 2014).

We have improved the accuracy of O_3 photodissociation rate calculations by including varying AOD and SSA in the TUV module, as described in Section 2.3.2. As a result, the increase in cloud cover reduced the shortwave radiation flux and photochemical formation rates of near-surface O_3, leading to decreased formation. Thus, the increase in near-surface temperature is often accompanied by an elevation in PBL height, enhanced cloud cover, precipitation, and reduced shortwave radiation. Moreover, higher wind speeds can enhance the dispersion of O_3 (Gorai et al., 2015).

The variations of MDA8 O_3, precipitation, clouds, shortwave flux (SWF), wind speed, temperature, and PBL height are presented individually in Figure 4~~6~~. The increase in SWF can accelerate O_3 formation through photochemistry (Jiang et al., 2012; Lelieveld and Crutzen, 1990). Therefore, the increased cloud fraction reduced surface O_3 by decreasing shortwave radiation, especially in NCP, FWP, YRD, and SCB in the PreG period (-10.63~-1.6 W/m^2). Furthermore, the enhanced precipitation in these regions (0.37~1.81 mm/day) reduced surface O_3 levels significantly. The significant increase in wind speed (0.17~0.26 m/s) also contributed to the reduction of surface O_3 in the NCP region (Table 4).

Another crucial factor is the elevated surface temperature (0~5 K), which intensified upward motion and raised the planetary boundary layer (PBL) height (0~500 m) across much of East Asia. Consequently, the increased temperature and PBL height could disperse surface-level O_3, thereby reducing its concentration.

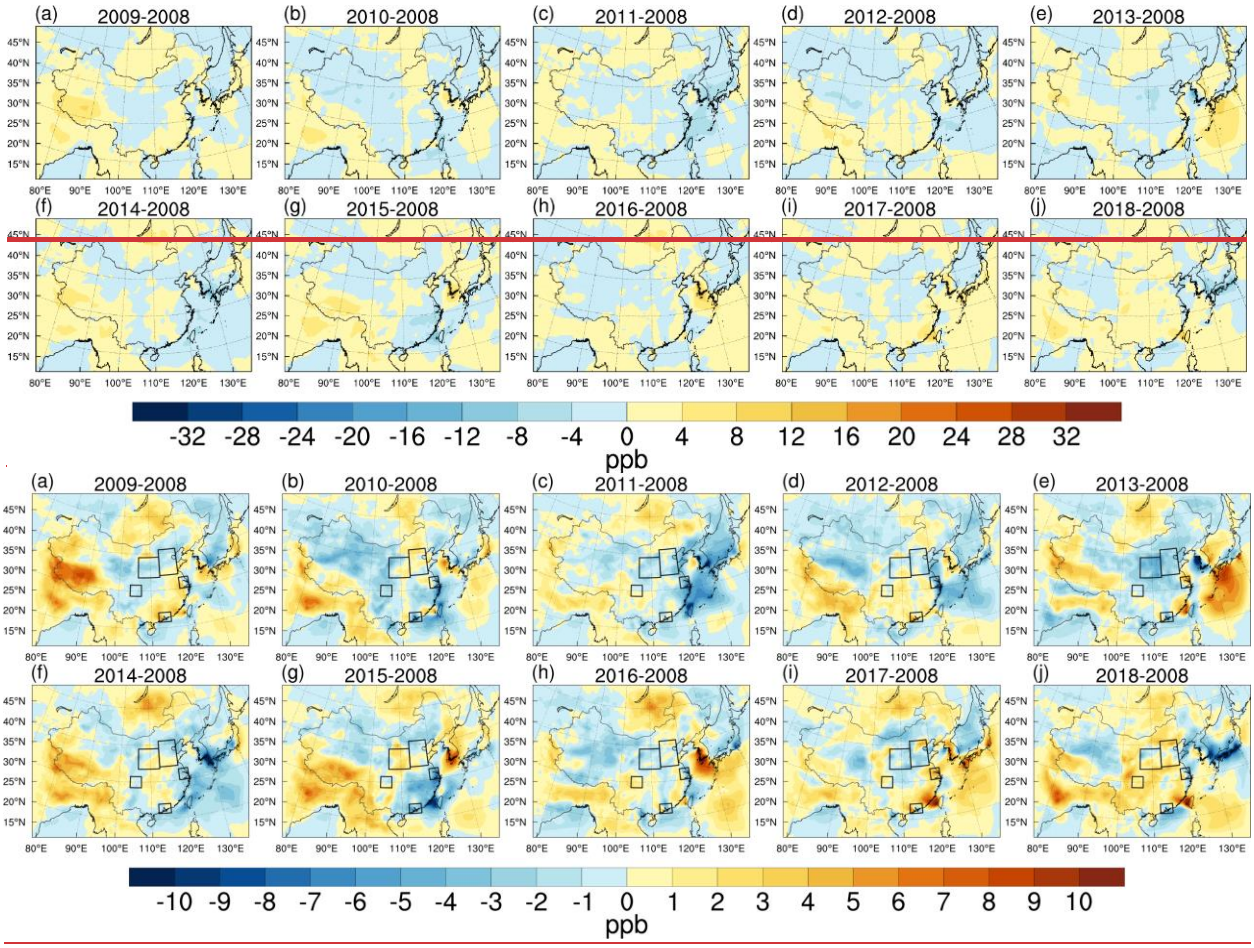

Figure 3~~5~~. The responds of the surface MDA8 O_3 mixing ratios (units: ppb) to variations in meteorological conditions during the summer monsoon period in 2009 (a), 2010 (b), 2011 (c), 2012 (d), 2013 (e), 2014 (f), 2015 (g), 2016 (h), 2017 (i) and 2018 (j) relative to 2008.

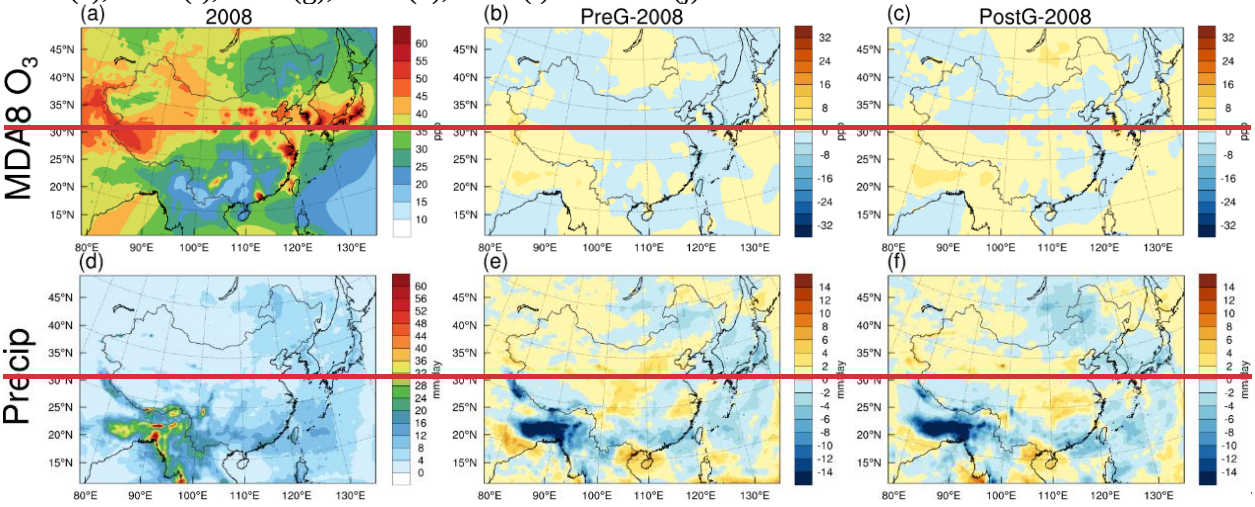

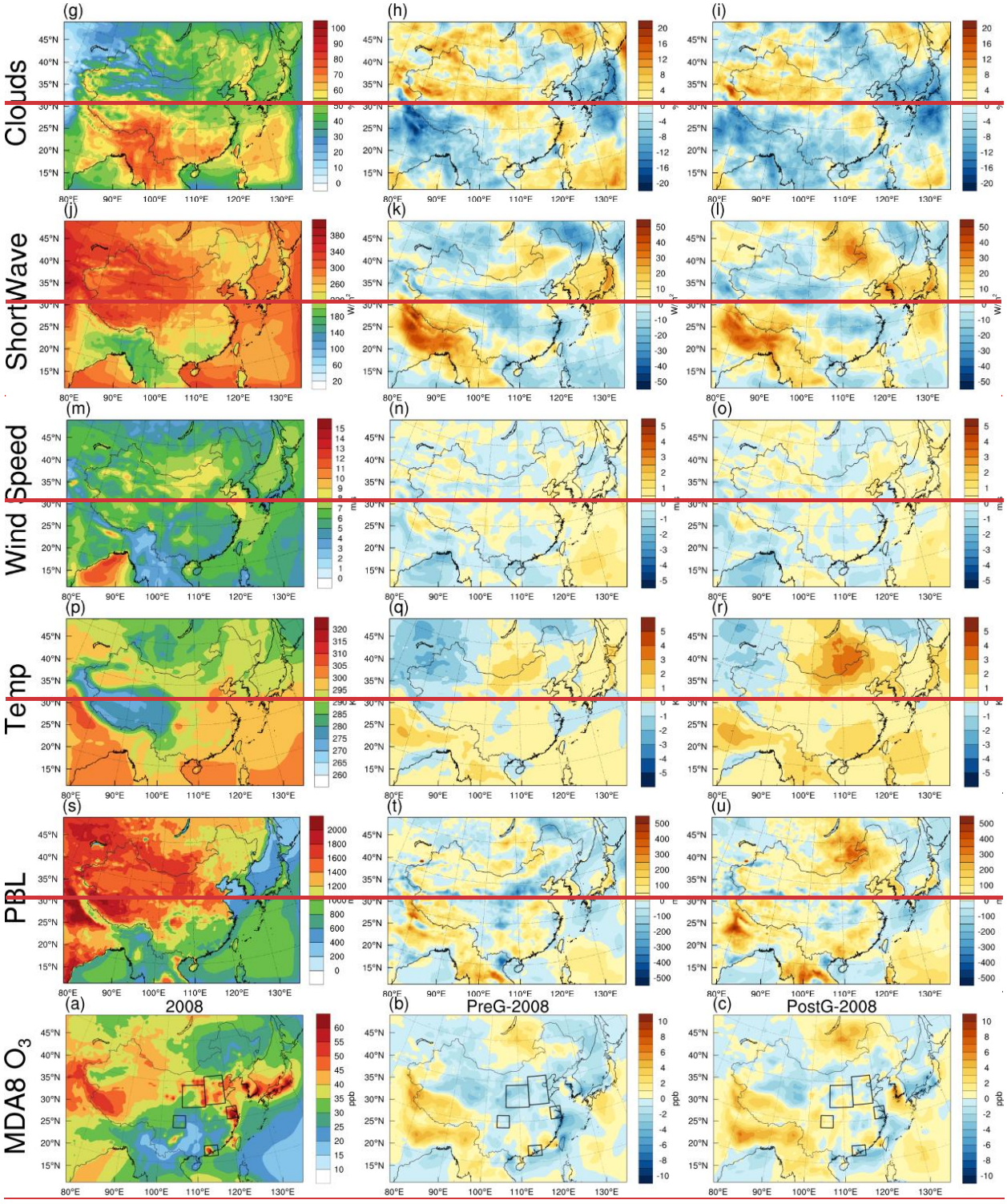
Clouds
ShortWave
Wind Speed
Temp
PBL
MDA8 O3
(a) 2008
(b) PreG-2008
(c) PostG-2008
(g)
(h)
(i)
(j)
(k)
(l)
(m)
(n)
(o)
(p)
(q)
(r)
(s)
(t)
(u)

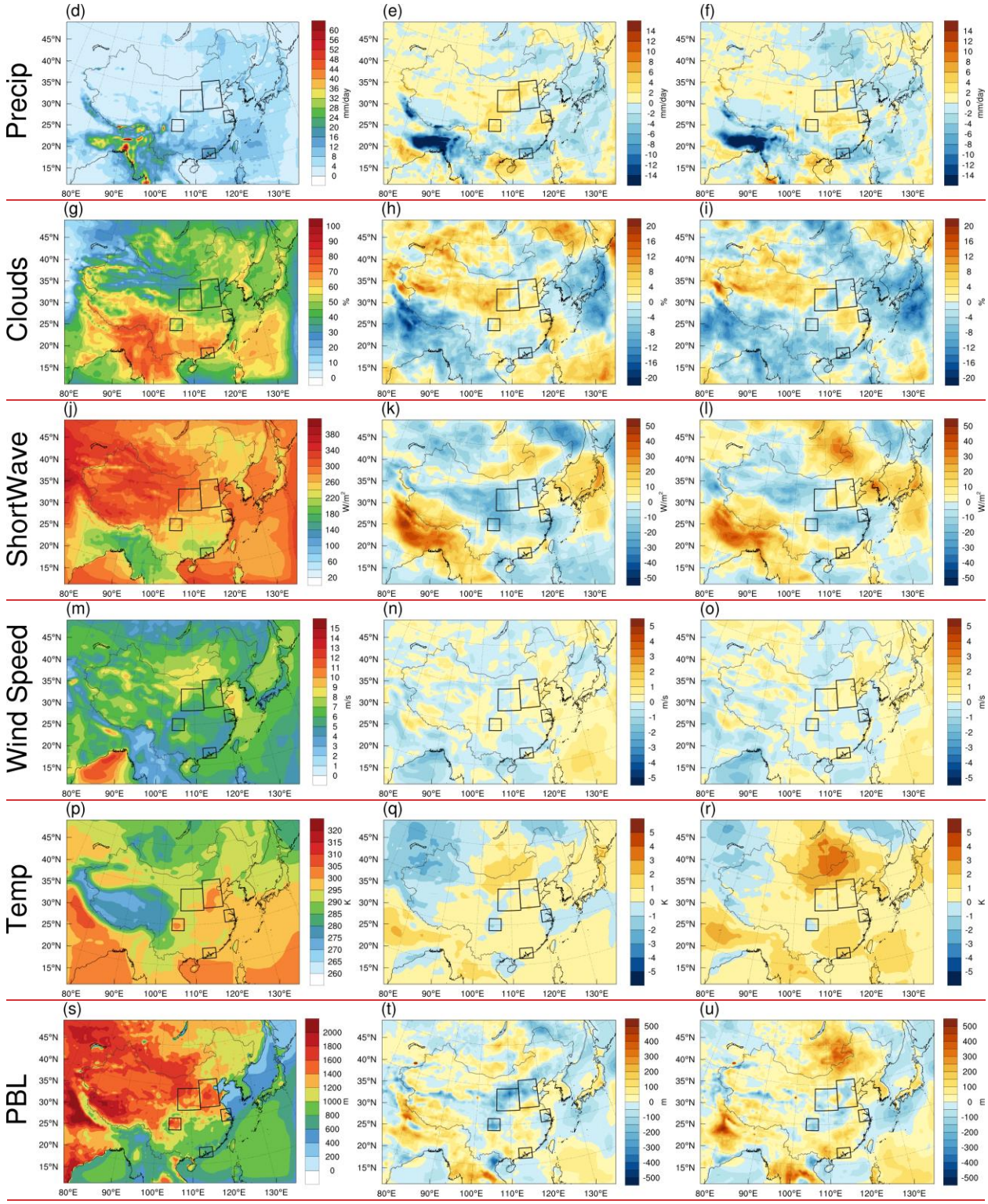

Figure 46. The MDA8 O_3 (a~c, units: ppb), precipitation (d~f, units: mm/day), clouds (g~i, units: %), shortwave flux (j~l, units: W/m^2), wind speed (m~o, units: m/s), temperature (p~r, units: K), and planetary boundary layer height (s~u, units: m) during the summer monsoon period in 2008 from the base simulations (the left column) and their responses due to variations in meteorological conditions in PreG (2009~2013, the central column) and PostG (2014~2018, the right column) relative to 2008.

Table 4~~3~~. Response of the MDA8 O_3 mixing ratios (units: ppb), precipitations (units: mm/day), clouds fraction (units: %), shortwave flux (units: W/m^2), wind speed (units: m/s), temperature (units: K), and planetary boundary layer height (units: m) to the changes in meteorological conditions over North China Plain, Fenwei Plain, Yangtze River Delta, Pearl River Delta, and Sichuan Basin during the summer monsoon period in PreG (2009~2013) and PostG (2014~2018) relative to 2008.

Regions	Period	MDA8 O_3 (ppb)	Precip (mm/day)	Clouds (%)	SWF (W/m^2)	Wind Speed (m/s)	Temp (K)	PBL (m)
NCP	PreG	-0.88	0.58	1.33	-3.04	0.17	0.32	-46.8
	PostG	-0.04	0.6	-0.93	3.06	0.26	0.6	-14.5
FWP	PreG	-1.41	1.68	2.86	-10.63	-0.06	0.1	-108.5
	PostG	-0.09	0.81	-0.94	-0.81	0.05	0.46	-15.3
YRD	PreG	-1.03	1.02	1.07	-1.6	0.18	-0.29	-33.9
	PostG	-0.96	0.48	-1.18	-4.85	-0.08	0.45	21.9
PRD	PreG	-0.23	-2.39	-1.93	2.24	-0.02	0.36	29.6
	PostG	-1.08	-3.24	-3.98	5.37	0.18	1.00	52.2
SCB	PreG	-0.41	1.81	0.59	-8.8	0.13	-0.58	-136.5
	PostG	0.71	0.37	-2.23	-3.2	-0.03	-0.14	-76

3.4 The effect of CO_2 in 2008~2018 ozone increase

The surface O_3 in southern China, which includes the YRD, PRD, and SCB regions, was characterized by high precipitation, temperatures, and vegetation cover, and was significantly impacted by CO_2 (Figure 5). Figures 6e and f demonstrate a marked rise in CO_2 levels across East Asia, particularly in eastern China, which was attributable to extensive human activity.

CO_2 is a significant driver of climate change and alterations in biogenic emissions. As shown in Figures 6 b and c, the impact of CO_2 on O_3 levels varies across locations, with a positive effect of 0.28~0.46 ppb along the southeastern coast of China but a negative influence of -0.51 to -0.11 ppb in the southwest and central China. CO_2 affects O_3 concentration by influencing both precipitation and isoprene emissions. In western and central China, CO_2 primarily affects O_3 concentration through its impact on precipitation (Table 5). Elevated CO_2 concentrations lead to increased precipitation (0.06~0.64 mm/day) in the FWP and SCB regions, resulting in a decrease in surface O_3 (up to -0.51 ppb). In eastern and southern coastal China, where vegetation is abundant, CO_2 has a greater impact on isoprene emissions. In the YRD region, decreased isoprene (-0.58 to -0.32 $\mu g/m^3$) and increased precipitations (0.09~0.13 mm/day) reduced MDA8 O_3 levels (0.09~0.14 ppb). In PRD, increased isoprene levels (0.31~0.92 $\mu g/m^3$) and decreased precipitations (-1.02~-0.33 mm/day) led to the enhancement of MDA8 O_3 (0.28~0.46 ppb).

~~And that was going to vary the surface O_3 concentrations. For instance, precipitation increased by 0.06 to 0.64 mm/day in the NCP, FWP, YRD, and SCB, where surface O_3 was reduced. In contrast, on the southeast coast of China (PRD), reduced precipitation accelerated the accumulation of MDA8 O_3 (0.28 to 0.46 ppb a^{-1}).~~

~~In the YRD region, the surface MDA8 O_3 was reduced (0.09–0.14 ppb a^{-1}), which attributed to the decreased isoprene. In contrast, the isoprene was increased by the elevated CO_2 concentrations on the southeast coast of China and then promoted the formation of surface O_3 (1–3 ppb) (Figure 8 b and c). In PRD, for example, the increased isoprene (0.31–0.92 $\mu g/m^3$ a^{-1})~~

~~contributed to MDA8 O_3 enhanced 0.28 to 0.46 ppb a^{-1}. Due to the lower temperature and vegetation cover, surface O_3 was insensitive to air CO_2 in the NCP.~~

In some years, the impact of changed CO_2 can be as significant as or even surpass that of anthropogenic emissions and meteorology (Figure 10). For example, in 2013, CO_2 caused an increase of 0.95 ppb in MDA8 O_3 in the YRD region, which exceeded that of anthropogenic emissions (0.87 ppb). Similarly, in the PRD region in 2012, the effect of CO_2, anthropogenic emissions, and meteorology was 1.41, 1.77, and 1.95 ppb, respectively. Even in the NCP in 2010, the impact of CO_2 (0.75 ppb) was comparable to that of anthropogenic emissions (1.5 ppb). In summary, CO_2 has a significant impact on surface O_3 concentrations by influencing radiation and isoprene emissions, with more prominent effects in regions with abundant vegetation.

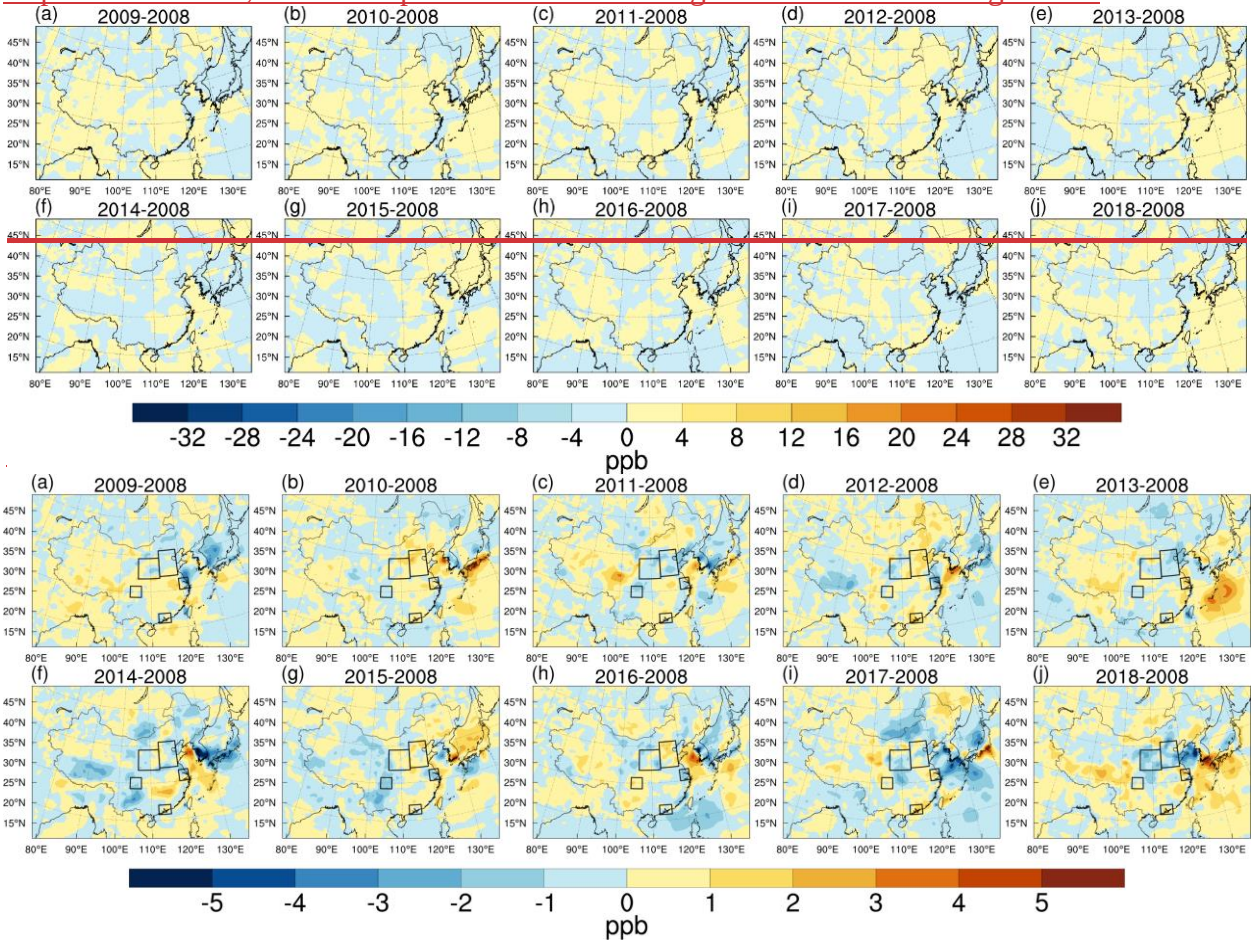

Figure 5~~7~~**.** Simulated responses of surface MDA8 O_3 mixing ratios (units: ppb) to the variations in CO_2 emissions during the summer monsoon period in 2009 (a), 2010 (b), 2011 (c), 2012 (d), 2013 ~~(e)~~I, 2014 (f), 2015 (g), 2016 (h), 2017 (i) and 2018 (j) relative to 2008.

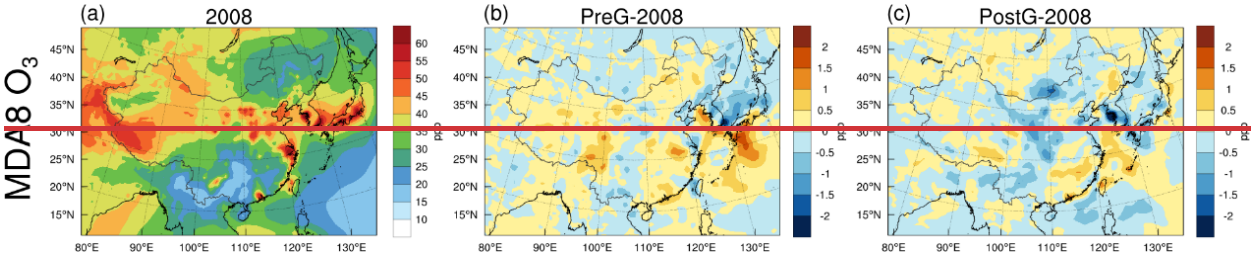

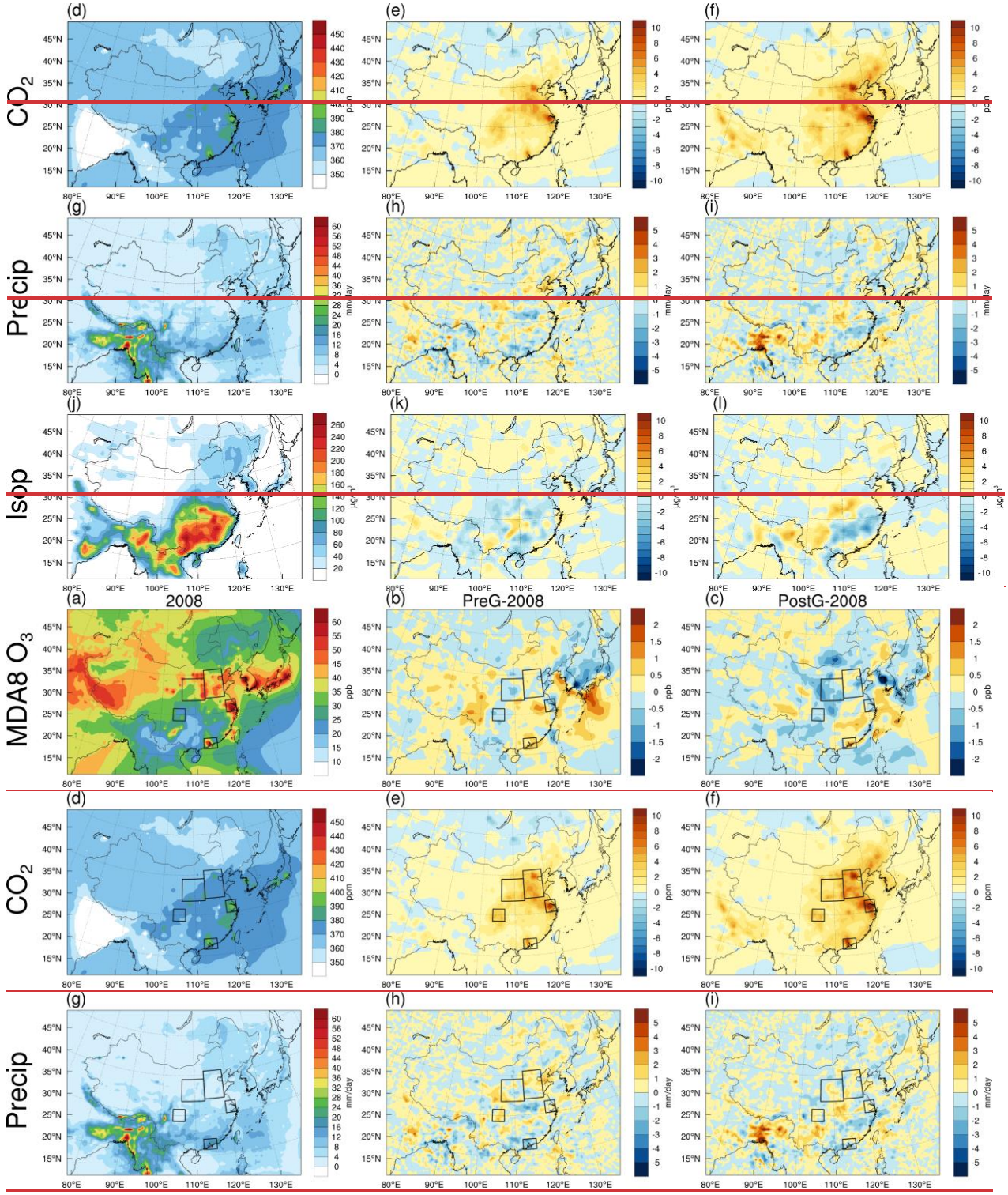
(d)
(e)
(f)
CO_2
ppm
(g)
(h)
(i)
Precip
mm/day
(j)
(k)
(l)
Isopp
μg/m³
(a)
2008
(b)
PreG-2008
(c)
PostG-2008
MDA8 O_3
ppb
(d)
(e)
(f)
CO_2
ppm
(g)
(h)
(i)
Precip
mm/day

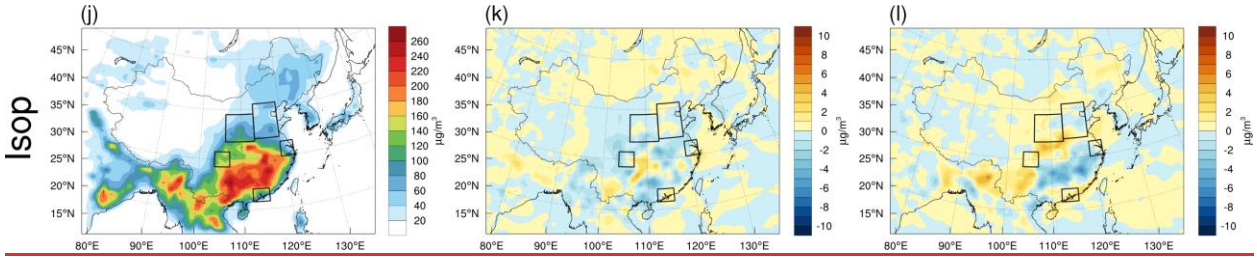

Figure ~~6~~8. The simulated averaged MDA8 O_3 (a~c, units: ppb), CO_2 (d~f, units: ppm), precipitation (g~i, units: mm/day), and isoprene mixing ratios (j~l, units: μg/m^3) in 2008 from the base simulations (the left column) and their changes due to variations in CO_2 emissions in PreG (2009~2013, the central column) and PostG (2014~2018, the right column) relative to 2008.

Table ~~5~~4. Simulated responses of MDA8 O_3 mixing ratios (units: ppb), CO_2 mixing ratios (units: ppm), precipitations (units: mm/day), and isoprene mixing ratios to the changes in CO_2 emissions over North China Plain, Fenwei Plain, Yangtze River Delta, Pearl River Delta, and Sichuan Basin in PreG (2009~2013) and PostG (2014~2018) relative to 2008.

Regions	Period	MDA8 O_3 (ppb)	CO_2 (ppm)	Precipitation (mm/day)	Isoprene (μ g/m^3)
NCP	PreG	0.07	3.19	0.27	-0.1
	PostG	-0.05	4.24	0.13	0.26
FWP	PreG	-0.11	1.70	0.21	-0.16
	PostG	-0.51	2.05	0.06	0.33
YRD	PreG	-0.09	4.1	0.13	-0.32
	PostG	-0.14	6.2	0.09	-0.58
PRD	PreG	0.46	1.97	-1.02	0.31
	PostG	0.28	3.20	-0.33	0.92
SCB	PreG	-0.30	2.80	0.64	-0.78
	PostG	-0.30	2.78	0.21	0.69

3.5 The effect of anthropogenic emission in 2008~2018 ozone increase

Finally, we calculated the anthropogenic emissions' effect on the 2008~2018 O_3 increase. Figure S8 and Table S1 illustrate that the levels of $PM_{2.5}$, PM_{10}, SO_2, CO, and OC emissions remained consistently high during the PreG period. However, a linear decrease in emissions was observed after the implementation of the Clean Air Action Plan in 2013. Prior to 2013, the emission of VOCs increased steadily but subsequently stabilized. Similarly, the emission of nitrogen oxides (NOx) exhibited an upward trend before 2013, but since then, the emissions have shown a linear decrease, with each subsequent year exhibiting lower levels of NOx emissions. In comparison to other species, the emissions of ammonia (NH_3) remained relatively stable from 2008 to 2018. Our analysis results of the emissions of different species align with those of Zheng et al. (2018), who computed the changes of each species in the MEIC inventory from 2010 to 2017.

Figure 7 illustrates that anthropogenic emissions have caused a notable increase in surface O_3 levels across most of China, particularly in megacity clusters. The impact of anthropogenic emissions on O_3 concentration ranged from 2.33 to 18.51 ppb in the five target regions.

Figure 8 and Table 6 illustrate that the changes in surface O_3 caused by anthropogenic emissions are similar in magnitude and spatial distribution to the changes in the base experiment. This suggests that anthropogenic emissions were the dominant factor driving the increase of surface O_3 in China from 2008 to 2018. Notably, a high-impact center of anthropogenic

emissions was simulated in North China, with the NCP region experiencing the most significant increase in surface O_3 (4.08~18.51 ppb), followed by the FWP, YRD, and SCB regions (4.10~11.5 ppb). In the PRD region, anthropogenic emissions led to a slight enhancement of O_3 by 2.33~5.74 ppb~~The O_3 was enhanced by 2.33–5.74 ppb a^{-1} in the PRD region due to the slight increase in air O_3 concentration~~.

The role of anthropogenic emissions increased linearly from 2008 to 2018, despite the implementation of the Clean Air Action Plan in 2013 (Table 6). For example, anthropogenic emissions significantly increased surface MDA8 O_3 in the NCP region (4.08 ppb~~ a^{-1}~~ in PreG and 18.51 ppb~~ a^{-1}~~ in PostG). Similarly, FWP experienced increases of 5.15 and 11.5 ppb ~~a^{-1}~~ in the PreG and PostG periods, respectively. In the SCB region, the surface MDA8 O_3 was mainly affected by variations in anthropogenic emissions due to the high levels of anthropogenic emissions in the complex basin topography. In the YRD and PRD regions, anthropogenic emissions resulted in changes to O_3 of 2.56~10.07 ppb~~ a^{-1}~~.

The reasons for this characteristic are multiple~~ic~~~~ed~~. Before 2013, the continuous increase in VOCs and NOx emissions (Figure S8 b, c) facilitated the rise of O_3 levels. Following the implementation of the Clean Air Action Plan in 2013, the emissions of VOCs and NOx were regulated. However, with the decrease in $PM_{2.5}$ levels, direct radiation increased, and scattered radiation decreased (Figure 9), thereby promoting the photochemical formation of O_3~~After aerosol reduction, the elevated photochemical formation rate significantly elevated surface O_3 level, especially in the PostG period~~ (Bian et al., 2007). In addition, t~~T~~he reduced NO emission weakened the titration effect (Figure S8 b), thus increasing surface O_3 (Li et al., 2022).

Our results are consistent with previous studies by Wang et al. (2019b) and Liu and Wang (2020b), which also showed the dominant and almost linear role of anthropogenic emissions in the increase of O_3 from 2013 to 2015 in four major Chinese cities (Beijing, Shanghai, Guangzhou, and Chengdu).

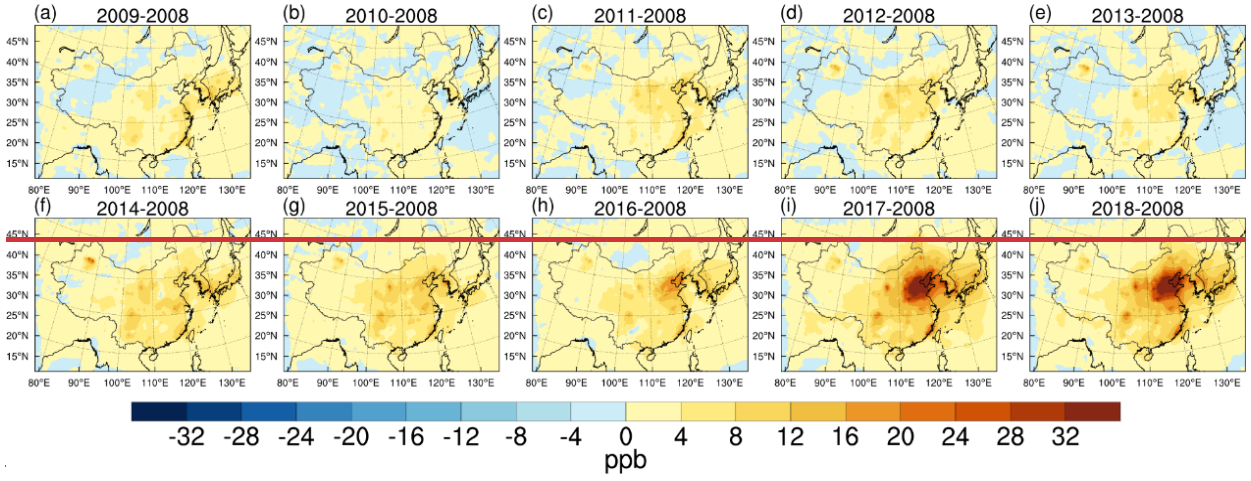

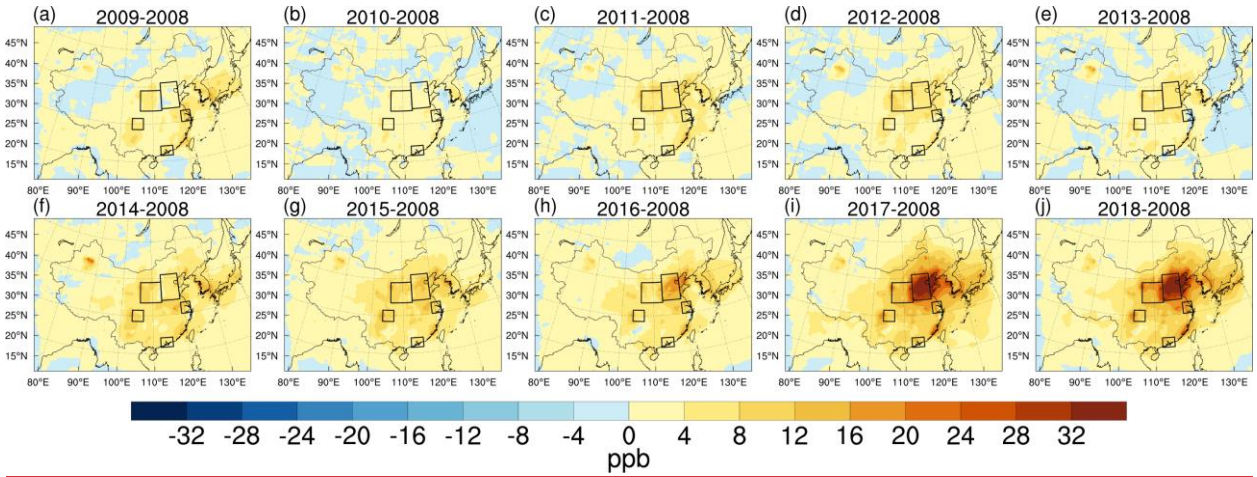

Figure 79. Simulated responses of the surface MDA8 O_3 mixing ratios (units: ppb) to variations in anthropogenic emissions in 2009 (a), 2010 (b), 2011 (c), 2012 (d), 2013 (e), 2014 (f), 2015 (g), 2016 (h), 2017 (i) and 2018 (j) relative to 2008.

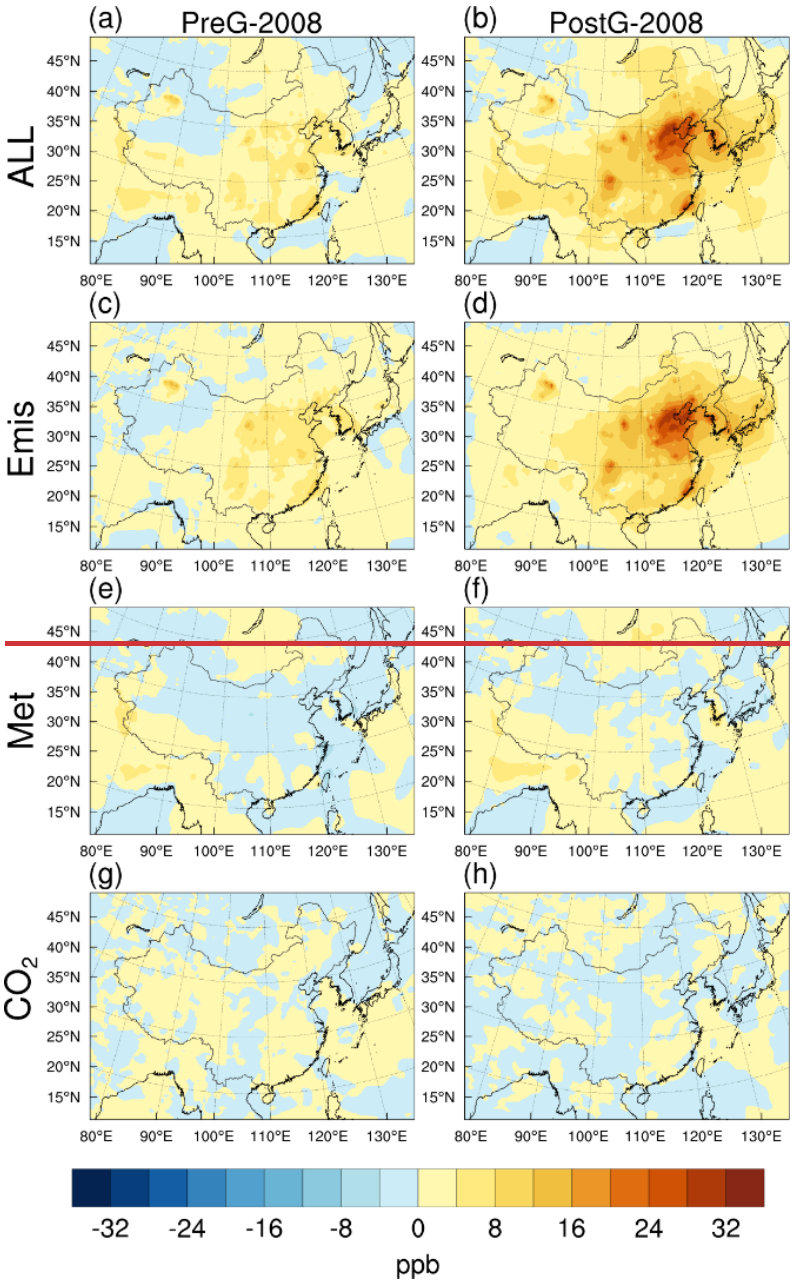
(a) PreG-2008
(b) PostG-2008
(c)
(d)
(e)
(f)
(g)
(h)
ALL
Emis
Met
CO_2
45°N
40°N
35°N
30°N
25°N
20°N
15°N
80°E
90°E
100°E
110°E
120°E
130°E
-32
-24
-16
-8
0
8
16
24
32
ppb

551

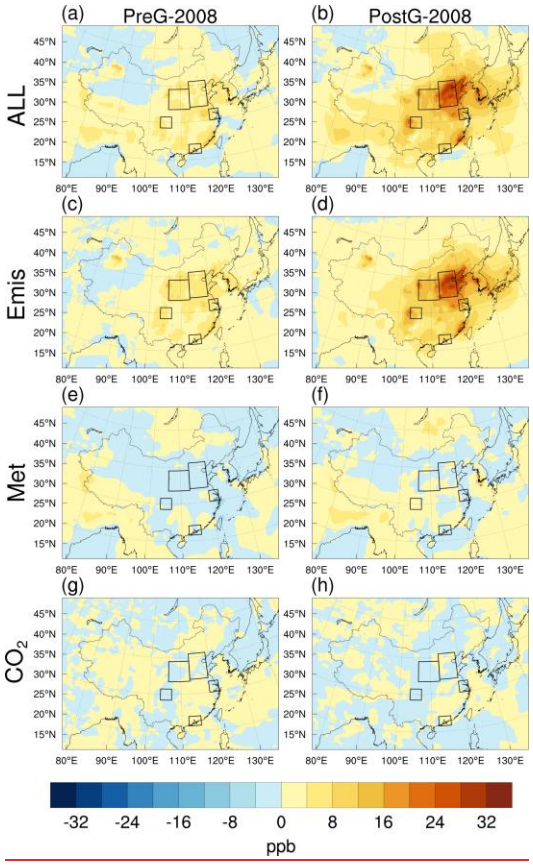

Figure 8~~10~~. Changes in the simulated surface MDA8 O_3 mixing ratios (units: ppb) from the base simulation (All, a,b); those due to variations in anthropogenic emissions (Emis, c,d), meteorological conditions (Met, e,f), and CO_2 emissions (CO_2, g,h) in PreG (2009~2013, the left column) and PostG (2014~2018, the right column) relative to 2008.

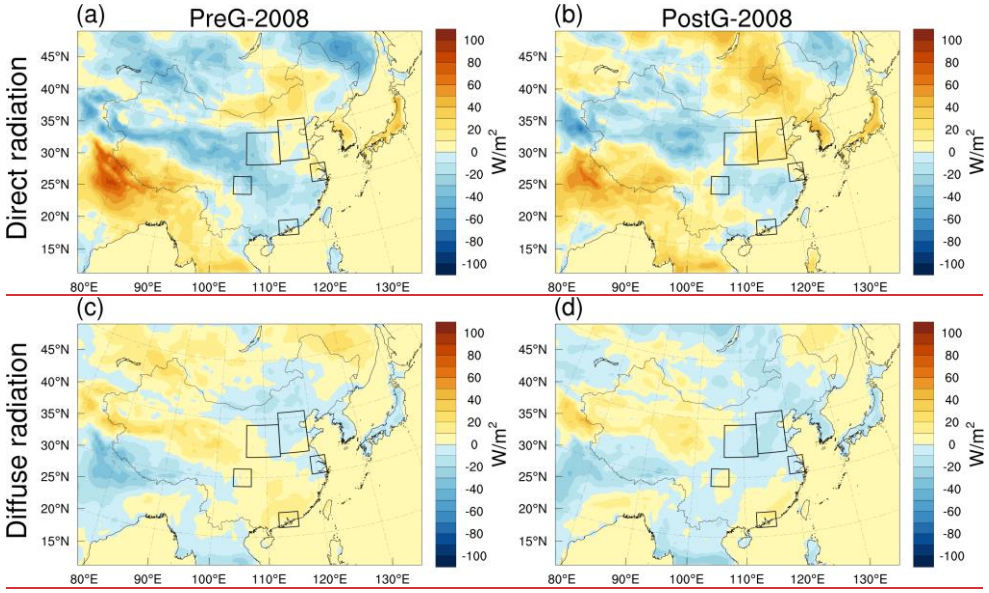

Figure 9. The variations of the surface direct radiation (a,b, units: W/m^2) and diffuse radiation (c,d, units: W/m^2) in the PreG (2009~2013, a,c) and PostG (2014~2018, b,d) period relative to 2008.

Table 6~~5~~. Simulated response of the MDA8 O_3 mixing ratios (units: ppb) to the changes in anthropogenic emissions (Emis), meteorological conditions (Met), and CO_2 emissions (CO_2) over North China Plain, Fenwei Plain, Yangtze River Delta, Pearl River Delta, and Sichuan Basin in PreG (2009~2013) and PostG (2014~2018) relative to 2008.

Regions	Period	ALL (ppb)	Emis (ppb)	Met (ppb)	CO_2 (ppb)
NCP	PreG	3.27	4.08	-0.88	0.07
	PostG	18.42	18.51	-0.04	-0.05
FWP	PreG	3.63	5.15	-1.41	-0.11
	PostG	10.9	11.5	-0.09	-0.51
YRD	PreG	2.98	4.10	-1.03	-0.09
	PostG	10.07	11.17	-0.96	-0.14
PRD	PreG	2.56	2.33	-0.23	0.46
	PostG	4.94	5.74	-1.08	0.28
SCB	PreG	3.67	4.38	-0.41	-0.30
	PostG	11.21	10.80	0.71	-0.30

3.6 Attribution analysis of ozone changes in 2008~2018

Finally, we presented an attribution diagram depicting the changes in O_3 concentration from 2008 to 2018. The total variation in O_3 concentration can be attributed to the combined effects of meteorological changes, changes in CO_2 concentration, and anthropogenic emissions (Figure 10).

The primary driver of the O_3 concentration variation from 2008 to 2018 was the changes in anthropogenic emissions, particularly in regions with high emissions, such as the NCP and FWP. Although the Clean Air Action Plan was implemented in 2013, it did not reduce the contribution of anthropogenic emissions to the O_3 increase. Even in the PostG period, with the development of urbanization and industrialization, the impact of changed anthropogenic emissions on O_3 has gradually become more prominent than changed meteorology and CO_2. The contribution of changed meteorology to O_3 was generally negative in the five regions, with a more significant impact in the YRD and PRD regions. This may be attributed to their proximity to the ocean and susceptibility to the summer monsoon influence. Changes in CO_2 concentration affected O_3 concentration by altering radiation and isoprene emissions, with a more significant impact in the YRD and PRD regions where vegetation was abundant. In some years, it even surpassed the effects of anthropogenic emissions. Therefore, we suggest that the influence of CO_2 concentration changes on O_3 concentration should be considered in regions with high vegetation coverage.

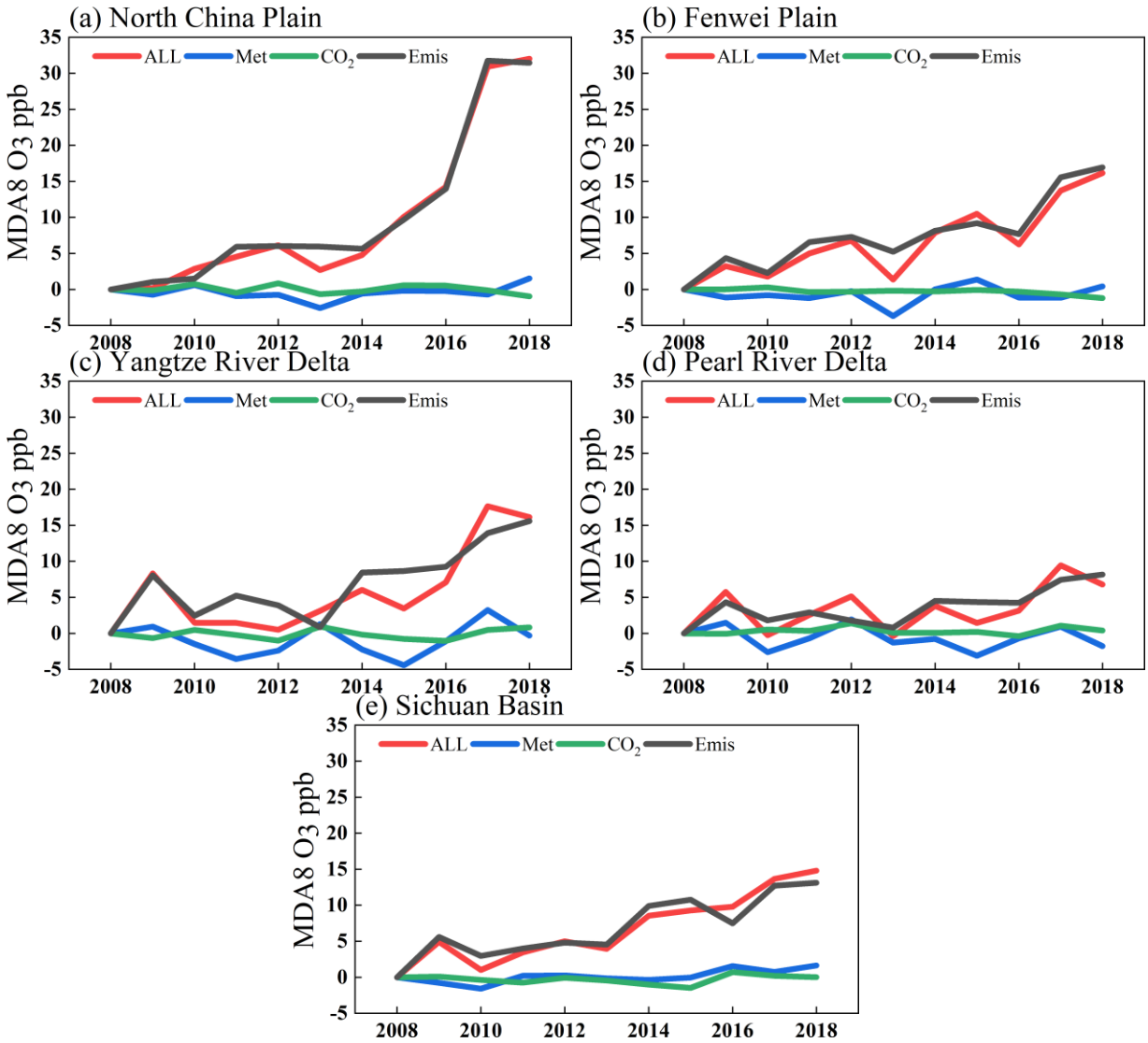

Figure 1~~0~~1. Interannual variations of the surface MDA8 O_3 mixing ratios (units: ppb) in the summer monsoon period (ALL) and the responses of variations in anthropogenic emissions (Emis), meteorological conditions (Met), and CO_2 emissions (CO_2) in (a) North China Plain, (b) Fenwei Plain, (c) Yangtze River Delta, (d) Pearl River Delta, and (e) Sichuan Basin in 2008~2018 relative to 2008.

~~In this work, the boundary conditions are kept consistent in base and sensitivity studies. We ignore the influence of boundary conditions on ozone due to the following reasons. First, in general, the regional model was coupled with the global model to get a more realistic influence from the boundary. However, for long-term climate-chemistry modeling, such coupling means a large computing resource. Second, the boundary conditions were derived from global models (Liu et al., 2017; Ban et al., 2014) and have to be prescribed in sensitive experiments. Third, fixed boundary conditions are widely used in some O_3 studies in China~~ (Liu and Wang, 2020a, b; Wang et al., 2019b)~~. Regional emissions are the major contributors of surface O_3 in China, accounting for 80% from May to August (Lu et al., 2019). Therefore, the uncertainty of fixed boundary conditions can be ignored at the current stage.~~

4 Conclusions

In this study. First, we improved the RegCM-Chem-YIBs model regarding the photolysis of O_3 and the radiation effect of CO_2 and O_3. Second, we assessed the impacts of anthropogenic

emissions, meteorological factors, and CO_2 on the surface O_3 increase in China during the EASM season from 2008 to 2018.

In the NCP and FWP regions. The increased surface O_3 (4.08~5.15 ppb~~a^{-1}~~ in PreG and 11.5~18.51 ppb~~a^{-1}~~ in PostG) was primarily attributed to the changes in anthropogenic emissions. Furthermore, the impact of anthropogenic emissions has increased linearly, despite the Clean Air Action Plan being implemented in 2013. In contrast, the effects of meteorological factors and CO_2 on O_3 were weak during the study period.

In the YRD and PRD regions. Ignoring the principal contributions of anthropogenic emissions, CO_2 significantly impacted the O_3 variations (-0.14~0.46 ppb~~a^{-1}~~). The varied CO_2 led to surface MDA8 O_3 changes of -0.09~-0.14 ppb ~~a^{-1}~~ in the YRD and 0.28~0.46 ppb ~~a^{-1}~~ in the PRD by modulating the isoprene emissions and precipitations. On the other hand, the meteorological conditions played a more significant role in surface O_3 than in NCP, FWP, and SCB regions, resulting in a decrease in MDA8 O_3 from 2008 to 2018 (-4.42~3.25 ppb~~a^{-1}~~).

In the SCB region. The increase in surface O_3 from 2008 to 2018 was primarily driven by variations in anthropogenic emissions. The effect of meteorological conditions was weak due to the high level of emissions and basin topography. However, the changes in CO_2 significantly impacted surface O_3 levels and were unfavorable to O_3 formation during the study period (-3.0 ppb ~~a^{-1}~~ in PreG and PostG).

In conclusion, anthropogenic emissions dominated the O_3 increase in China from 2008 to 2018, and the effects of meteorological conditions on surface O_3 could be more significant in some regions. Furthermore, we emphasize the significance of CO_2 emissions, particularly in southern China, as a critical contributor to O_3 variations. Therefore, it is vital to consider CO_2 variability in future predictions of O_3 concentrations. Such consideration would be helpful for designing long-term O_3 control policies.

Data availability

ERA-Interim data are available at https://apps.ecmwf.int/datasets/data/interim-full-daily/. MEICv1.3 data are available at http://meicmodel.org/?page_id=560. CarbonTracker data are available at https://gml.noaa.gov/aftp/products/carbontracker/co2/CT2019/. OISST data are available at https://downloads.psl.noaa.gov/Datasets/noaa.oisst.v2/. WDCGG CO_2 data are available at https://gaw.kishou.go.jp/search/gas_species/co2/latest/. CNEMC data are available at http://www.cnemc.cn/. only available in Chinese, last access 1 May 2022.

Author contributions

642 **DM:** performed experiments; **TW:** designed the overall research; **HW, YQ, JL, JaL, and**
643 **SL** reviewed and edited the manuscript; **BL, ML, and MX** contributed to the development of the
644 RegCM-Chem-YIBs model.
645
646 **Competing interests:**
647 The contact author has declared that none of the authors has any competing interests.
648
649 **Disclaimer**
650 Publisher's note: Copernicus Publications remains neutral with regard to jurisdictional claims in
651 published maps and institutional affiliations.
652
653 **Financial support**
654 This work was supported by the National Natural Science Foundation of China (42077192,
655 41621005), the National Key Basic Research & Development Program of China
656 (2020YFA0607802, 2019YFC0214603), Creative talent exchange program for foreign experts in
657 the Belt and Road countries, and the Emory University-Nanjing University Collaborative
658 Research Grant.

References

Accadia, C., Zecchetto, S., Lavagnini, A., and Speranza, A.: Comparison of 10-m wind forecasts from a regional area model and QuikSCAT Scatterometer wind observations over the Mediterranean Sea, Monthly Weather Review, 135, 1945-1960,https://doi.org/10.1175/mwr3370.1, 2007.

Anwar, S. A., Zakey, A. S., Robaa, S. M., and Wahab, M. M. A.: The influence of two land-surface hydrology schemes on the regional climate of Africa using the RegCM4 model (vol 136, pg 1535, 2019), Theoretical and Applied Climatology, 136, 1549-1550,https://doi.org/10.1007/s00704-018-2588-0, 2019.

Ashmore, M. R. and Bell, J. N. B.: THE ROLE OF OZONE IN GLOBAL CHANGE, Annals of Botany, 67, 39-48,https://doi.org/10.1093/oxfordjournals.aob.a088207, 1991.

Ballantyne, A. P., Alden, C. B., Miller, J. B., Tans, P. P., and White, J. W. C.: Increase in observed net carbon dioxide uptake by land and oceans during the past 50 years, Nature, 488, 70-+,https://doi.org/10.1038/nature11299, 2012.

Balsamo, G., Albergel, C., Beljaars, A., Boussetta, S., Brun, E., Cloke, H., Dee, D., Dutra, E., Munoz-Sabater, J., Pappenberger, F., de Rosnay, P., Stockdale, T., and Vitart, F.: ERA-Interim/Land: a global land surface reanalysis data set, Hydrology and Earth System Sciences, 19, 389-407,https://doi.org/10.5194/hess-19-389-2015, 2015.

Ban, N., Schmidli, J., and Schar, C.: Evaluation of the convection-resolving regional climate modeling approach in decade-long simulations, Journal of Geophysical Research-Atmospheres, 119,https://doi.org/10.1002/2014jd021478, 2014.

Bian, H., Han, S. Q., Tie, X. X., Sun, M. L., and Liu, A. X.: Evidence of impact of aerosols on surface ozone concentration in Tianjin, China, Atmospheric Environment, 41, 4672-4681,https://doi.org/10.1016/j.atmosenv.2007.03.041, 2007.

Borg, I., Groenen, P. J. F., Jehn, K. A., Bilsky, W., and Schwartz, S. H.: Embedding the Organizational Culture Profile Into Schwartz's Theory of Universals in Values, Journal of Personnel Psychology, 10, 1-12,https://doi.org/10.1027/1866-5888/a000028, 2011.

Carvalho, D., Rocha, A., Gomez-Gesteira, M., and Santos, C.: A sensitivity study of the WRF model in wind simulation for an area of high wind energy, Environmental Modelling & Software, 33, 23-34,https://doi.org/10.1016/j.envsoft.2012.01.019, 2012.

Cassola, F. and Burlando, M.: Wind speed and wind energy forecast through Kalman filtering of Numerical Weather Prediction model output, Applied Energy, 99, 154-166,https://doi.org/10.1016/j.apenergy.2012.03.054, 2012.

Chen, Z., Zhuang, Y., Xie, X., Chen, D., Cheng, N., Yang, L., and Li, R.: Understanding long-term variations of meteorological influences on ground ozone concentrations in Beijing During 2006-2016, Environmental Pollution, 245, 29-37,https://doi.org/10.1016/j.envpol.2018.10.117, 2019.

Cheng, N., Li, R., Xu, C., Chen, Z., Chen, D., Meng, F., Cheng, B., Ma, Z., Zhuang, Y., He, B., and Gao, B.: Ground ozone variations at an urban and a rural station in Beijing from 2006 to 2017: Trend, meteorological influences and formation regimes, Journal of Cleaner Production, 235, 11-20,https://doi.org/10.1016/j.jclepro.2019.06.204, 2019.

Collins, W. D., Bitz, C. M., Blackmon, M. L., Bonan, G. B., Bretherton, C. S., Carton, J. A., Chang, P., Doney, S. C., Hack, J. J., Henderson, T. B., Kiehl, J. T., Large, W. G., McKenna, D. S., Santer, B. D., and Smith, R. D.: The Community Climate System Model version 3 (CCSM3), Journal of Climate, 19, 2122-2143,https://doi.org/10.1175/jcli3761.1, 2006.

Dang, R., Liao, H., and Fu, Y.: Quantifying the anthropogenic and meteorological influences on summertime surface ozone in China over 2012-2017, Science of the Total Environment, 754,https://doi.org/10.1016/j.scitotenv.2020.142394, 2021.

Decker, M. and Zeng, X. B.: Impact of Modified Richards Equation on Global Soil Moisture Simulation in the Community Land Model (CLM3.5), Journal of Advances in Modeling Earth Systems, 1,https://doi.org/10.3894/james.2009.1.5, 2009.

Duan, X.-t., Cao, N.-w., Wang, X., Zhang, Y.-x., Liang, J.-s., Yang, S.-p., and Song, X.-y.: Characteristics Analysis of the Surface Ozone Concentration of China in 2015, Huanjing Kexue, 38, 4976-4982,https://doi.org/10.13227/j.hjkx.201703045, 2017.

Fang, Y., Fiore, A. M., Horowitz, L. W., Gnanadesikan, A., Held, I., Chen, G., Vecchi, G., and Levy, H.: The impacts of changing transport and precipitation on pollutant distributions in a future climate, Journal of Geophysical Research-Atmospheres, 116,https://doi.org/10.1029/2011jd015642, 2011.

Fiore, A. M., Levy, H., II, and Jaffe, D. A.: North American isoprene influence on intercontinental ozone pollution, Atmospheric Chemistry and Physics, 11, 1697-1710,https://doi.org/10.5194/acp-11-1697-2011, 2011.

Gao, M., Carmichael, G. R., Wang, Y., Saide, P. E., Yu, M., Xin, J., Liu, Z., and Wang, Z.: Modeling study of the 2010 regional haze event in the North China Plain, Atmospheric Chemistry and Physics, 16, 1673-1691,https://doi.org/10.5194/acp-16-1673-2016, 2016.

Gao, M., Gao, J., Zhu, B., Kumar, R., Lu, X., Song, S., Zhang, Y., Jia, B., Wang, P., Beig, G., Hu, J., Ying, Q., Zhang, H., Sherman, P., and McElroy, M. B.: Ozone pollution over China and India: seasonality and sources, Atmospheric Chemistry and Physics, 20, 4399-4414,https://doi.org/10.5194/acp-20-4399-2020, 2020.

Gauss, M., Myhre, G., Pitari, G., Prather, M. J., Isaksen, I. S. A., Berntsen, T. K., Brasseur, G. P., Dentener, F. J., Derwent, R. G., Hauglustaine, D. A., Horowitz, L. W., Jacob, D. J., Johnson, M., Law, K. S., Mickley, L. J., Muller, J. F., Plantevin, P. H., Pyle, J. A., Rogers, H. L., Stevenson, D. S., Sundet, J. K., van Weele, M., and Wild, O.: Radiative forcing in the 21st century due to ozone changes in the troposphere and the lower stratosphere, Journal of Geophysical Research-Atmospheres, 108,https://doi.org/10.1029/2002jd002624, 2003.

Giorgi, F. and Mearns, L. O.: Introduction to special section: Regional climate modeling revisited, Journal of Geophysical Research-Atmospheres, 104, 6335-6352,https://doi.org/10.1029/98jd02072, 1999.

Giorgi, F., Coppola, E., Solmon, F., Mariotti, L., Sylla, M. B., Bi, X., Elguindi, N., Diro, G. T., Nair, V., Giuliani, G., Turuncoglu, U. U., Cozzini, S., Guettler, I., O'Brien, T. A., Tawfik, A. B., Shalaby, A., Zakey, A. S., Steiner, A. L., Stordal, F., Sloan, L. C., and Brankovic, C.: RegCM4: model description and preliminary tests over multiple CORDEX domains, Climate Research, 52, 7-29,https://doi.org/10.3354/cr01018, 2012.

Gorai, A. K., Tuluri, F., Tchounwou, P. B., and Ambinakudige, S.: Influence of local meteorology and NO2 conditions on ground-level ozone concentrations in the eastern part of Texas, USA, Air Quality Atmosphere and Health, 8, 81-96,https://doi.org/10.1007/s11869-014-0276-5, 2015.

Grell, G. A.: PROGNOSTIC EVALUATION OF ASSUMPTIONS USED BY CUMULUS PARAMETERIZATIONS, Monthly Weather Review, 121, 764-787,https://doi.org/10.1175/1520-0493(1993)121<0764:Peoaub>2.0.Co;2, 1993.

Guan, Y. R., Shan, Y. L., Huang, Q., Chen, H. L., Wang, D., and Hubacek, K.: Assessment to

751 China's Recent Emission Pattern Shifts, Earths Future,
752 9,https://doi.org/10.1029/2021ef002241, 2021.
753 Guenther, A. B., Monson, R. K., and Fall, R.: ISOPRENE AND MONOTERPENE EMISSION
754 RATE VARIABILITY - OBSERVATIONS WITH EUCALYPTUS AND EMISSION
755 RATE ALGORITHM DEVELOPMENT, Journal of Geophysical Research-Atmospheres,
756 96, 10799-10808,https://doi.org/10.1029/91jd00960, 1991.
757 Guo, J. P., Miao, Y. C., Zhang, Y., Liu, H., Li, Z. Q., Zhang, W. C., He, J., Lou, M. Y., Yan, Y.,
758 Bian, L. G., and Zhai, P.: The climatology of planetary boundary layer height in China
759 derived from radiosonde and reanalysis data, Atmospheric Chemistry and Physics, 16,
760 13309-13319,https://doi.org/10.5194/acp-16-13309-2016, 2016.
761 Haman, C. L., Couzo, E., Flynn, J. H., Vizuete, W., Heffron, B., and Lefer, B. L.: Relationship
762 between boundary layer heights and growth rates with ground-level ozone in Houston,
763 Texas, Journal of Geophysical Research-Atmospheres, 119, 6230-
764 6245,https://doi.org/10.1002/2013jd020473, 2014.
765 Han, H., Liu, J., Shu, L., Wang, T., and Yuan, H.: Local and synoptic meteorological influences
766 on daily variability in summertime surface ozone in eastern China, Atmospheric
767 Chemistry and Physics, 20, 203-222,https://doi.org/10.5194/acp-20-203-2020, 2020.
768 He, J. W., Wang, Y. X., Hao, J. M., Shen, L. L., and Wang, L.: Variations of surface O-3 in
769 August at a rural site near Shanghai: influences from the West Pacific subtropical high
770 and anthropogenic emissions, Environmental Science and Pollution Research, 19, 4016-
771 4029,https://doi.org/10.1007/s11356-012-0970-5, 2012.
772 Heald, C. L., Wilkinson, M. J., Monson, R. K., Alo, C. A., Wang, G. L., and Guenther, A.:
773 Response of isoprene emission to ambient CO2 changes and implications for global
774 budgets, Global Change Biology, 15, 1127-1140,https://doi.org/10.1111/j.1365-
775 2486.2008.01802.x, 2009.
776 Hoffmann, L., Gunther, G., Li, D., Stein, O., Wu, X., Griessbach, S., Heng, Y., Konopka, P.,
777 Muller, R., Vogel, B., and Wright, J. S.: From ERA-Interim to ERA5: the considerable
778 impact of ECMWF's next-generation reanalysis on Lagrangian transport simulations,
779 Atmospheric Chemistry and Physics, 19, 3097-3124,https://doi.org/10.5194/acp-19-3097-
780 2019, 2019.
781 Hong, C. P., Zhang, Q., He, K. B., Guan, D. B., Li, M., Liu, F., and Zheng, B.: Variations of
782 China's emission estimates: response to uncertainties in energy statistics, Atmospheric
783 Chemistry and Physics, 17, 1227-1239,https://doi.org/10.5194/acp-17-1227-2017, 2017.
784 IPCC (Ed.) Intergovernmental Panel on Climate Change (IPCC) (2021), the Physical Science
785 Basis. Contribution of Working Group I to the Sixth Assessment Report of the
786 Intergovernmental Panel on Climate Change, Cambridge University Press,Cambridge,
787 United Kingdom and New York, NY, USA. , 2021.
788 Jacob, D. J. and Winner, D. A.: Effect of climate change on air quality, Atmospheric
789 Environment, 43, 51-63,https://doi.org/10.1016/j.atmosenv.2008.09.051, 2009.
790 Jacobs, N., Simpson, W. R., Graham, K. A., Holmes, C., Hase, F., Blumenstock, T., Tu, Q., Frey,
791 M., Dubey, M. K., Parker, H. A., Wunch, D., Kivi, R., Heikkinen, P., Notholt, J., Petri, C.,
792 and Warneke, T.: Spatial distributions of X-CO2 seasonal cycle amplitude and phase over
793 northern high-latitude regions, Atmospheric Chemistry and Physics, 21, 16661-
794 16687,https://doi.org/10.5194/acp-21-16661-2021, 2021.
795 Jiang, X., Wiedinmyer, C., and Carlton, A. G.: Aerosols from Fires: An Examination of the
796 Effects on Ozone Photochemistry in the Western United States, Environmental Science &

Technology, 46, 11878-11886,https://doi.org/10.1021/es301541k, 2012.
KhayatianYazdi, F., Kamali, G., Mirrokni, S. M., and Memarian, M. H.: Sensitivity evaluation of the different physical parameterizations schemes in regional climate model RegCM4.5 for simulation of air temperature and precipitation over North and West of Iran, Dynamics of Atmospheres and Oceans, 93,https://doi.org/10.1016/j.dynatmoce.2020.101199, 2021.
Kong, L., Tang, X., Zhu, J., Wang, Z., Li, J., Wu, H., Wu, Q., Chen, H., Zhu, L., Wang, W., Liu, B., Wang, Q., Chen, D., Pan, Y., Song, T., Li, F., Zheng, H., Jia, G., Lu, M., Wu, L., and Carmichael, G. R.: A 6-year-long (2013-2018) high-resolution air quality reanalysis dataset in China based on the assimilation of surface observations from CNEMC, Earth System Science Data, 13, 529-570,https://doi.org/10.5194/essd-13-529-2021, 2021.
Lee, Y. C., Shindell, D. T., Faluvegi, G., Wenig, M., Lam, Y. F., Ning, Z., Hao, S., and Lai, C. S.: Increase of ozone concentrations, its temperature sensitivity and the precursor factor in South China, Tellus Series B-Chemical and Physical Meteorology, 66,https://doi.org/10.3402/tellusb.v66.23455, 2014.
Lefer, B. L., Shetter, R. E., Hall, S. R., Crawford, J. H., and Olson, J. R.: Impact of clouds and aerosols on photolysis frequencies and photochemistry during TRACE-P: 1. Analysis using radiative transfer and photochemical box models, Journal of Geophysical Research-Atmospheres, 108,https://doi.org/10.1029/2002jd003171, 2003.
Lelieveld, J. and Crutzen, P. J.: INFLUENCES OF CLOUD PHOTOCHEMICAL PROCESSES ON TROPOSPHERIC OZONE, Nature, 343, 227-233,https://doi.org/10.1038/343227a0, 1990.
Li, J., Chen, X. S., Wang, Z. F., Du, H. Y., Yang, W. Y., Sun, Y. L., Hu, B., Li, J. J., Wang, W., Wang, T., Fu, P. Q., and Huang, H. L.: Radiative and heterogeneous chemical effects of aerosols on ozone and inorganic aerosols over East Asia, Science of the Total Environment, 622, 1327-1342,https://doi.org/10.1016/j.scitotenv.2017.12.041, 2018.
Li, K., Jacob, D. J., Liao, H., Shen, L., Zhang, Q., and Bates, K. H.: Anthropogenic drivers of 2013-2017 trends in summer surface ozone in China, Proceedings of the National Academy of Sciences of the United States of America, 116, 422-427,https://doi.org/10.1073/pnas.1812168116, 2019.
Li, K., Jacob, D. J., Shen, L., Lu, X., De Smedt, I., and Liao, H.: Increases in surface ozone pollution in China from 2013 to 2019: anthropogenic and meteorological influences, Atmospheric Chemistry and Physics, 20, 11423-11433,https://doi.org/10.5194/acp-20-11423-2020, 2020.
Li, R., Zhang, M., Chen, L., Kou, X., and Skorokhod, A.: CMAQ simulation of atmospheric CO2 concentration in East Asia: Comparison with GOSAT observations and ground measurements, Atmospheric Environment, 160, 176-185,https://doi.org/10.1016/j.atmosenv.2017.03.056, 2017.
Li, X. B., Yuan, B., Parrish, D. D., Chen, D. H., Song, Y. X., Yang, S. X., Liu, Z. J., and Shao, M.: Long-term trend of ozone in southern China reveals future mitigation strategy for air pollution, Atmospheric Environment, 269,https://doi.org/10.1016/j.atmosenv.2021.118869, 2022.
Lin, J.-T., Patten, K. O., Hayhoe, K., Liang, X.-Z., and Wuebbles, D. J.: Effects of future climate and biogenic emissions changes on surface ozone over the United States and China, Journal of Applied Meteorology and Climatology, 47, 1888-1909,https://doi.org/10.1175/2007jamc1681.1, 2008.

Liu, C. H., Ikeda, K., Rasmussen, R., Barlage, M., Newman, A. J., Prein, A. F., Chen, F., Chen, L., Clark, M., Dai, A. G., Dudhia, J., Eidhammer, T., Gochis, D., Gutmann, E., Kurkute, S., Li, Y. P., Thompson, G., and Yates, D.: Continental-scale convection-permitting modeling of the current and future climate of North America, Climate Dynamics, 49, 71-95,https://doi.org/10.1007/s00382-016-3327-9, 2017.

Liu, H., Liu, S., Xue, B., Lv, Z., Meng, Z., Yang, X., Xue, T., Yu, Q., and He, K.: Ground-level ozone pollution and its health impacts in China, Atmospheric Environment, 173, 223-230,https://doi.org/10.1016/j.atmosenv.2017.11.014, 2018a.

Liu, L., Zhou, L., Zhang, X., Wen, M., Zhang, F., Yao, B., and Fang, S.: The characteristics of atmospheric CO2 concentration variation of four national background stations in China, Science in China Series D-Earth Sciences, 52, 1857-1863,https://doi.org/10.1007/s11430-009-0143-7, 2009.

Liu, Y. and Wang, T.: Worsening urban ozone pollution in China from 2013 to 2017-Part 1: The complex and varying roles of meteorology, Atmospheric Chemistry and Physics, 20, 6305-6321,https://doi.org/10.5194/acp-20-6305-2020, 2020a.

Liu, Y. and Wang, T.: Worsening urban ozone pollution in China from 2013 to 2017-Part 2: The effects of emission changes and implications for multi-pollutant control, Atmospheric Chemistry and Physics, 20, 6323-6337,https://doi.org/10.5194/acp-20-6323-2020, 2020b.

Liu, Z., Liu, Y., Wang, S., Yang, X., Wang, L., Baig, M. H. A., Chi, W., and Wang, Z.: Evaluation of Spatial and Temporal Performances of ERA-Interim Precipitation and Temperature in Mainland China, Journal of Climate, 31, 4347-4365,https://doi.org/10.1175/jcli-d-17-0212.1, 2018b.

Lu, H., Yi, S., Liu, Z., Mason, J. A., Jiang, D., Cheng, J., Stevens, T., Xu, Z., Zhang, E., Jin, L., Zhang, Z., Guo, Z., Wang, Y., and Otto-Bliesner, B.: Variation of East Asian monsoon precipitation during the past 21 k.y. and potential CO2 forcing, Geology, 41, 1023-1026,https://doi.org/10.1130/g34488.1, 2013.

Lu, X., Zhang, L., Wang, X. L., Gao, M., Li, K., Zhang, Y. Z., Yue, X., and Zhang, Y. H.: Rapid Increases in Warm-Season Surface Ozone and Resulting Health Impact in China Since 2013, Environmental Science & Technology Letters, 7, 240-247,https://doi.org/10.1021/acs.estlett.0c00171, 2020.

Lu, X., Hong, J., Zhang, L., Cooper, O. R., Schultz, M. G., Xu, X., Wang, T., Gao, M., Zhao, Y., and Zhang, Y.: Severe Surface Ozone Pollution in China: A Global Perspective, Environmental Science & Technology Letters, 5, 487-494,https://doi.org/10.1021/acs.estlett.8b00366, 2018.

Lu, X., Zhang, L., Chen, Y. F., Zhou, M., Zheng, B., Li, K., Liu, Y. M., Lin, J. T., Fu, T. M., and Zhang, Q.: Exploring 2016-2017 surface ozone pollution over China: source contributions and meteorological influences, Atmospheric Chemistry and Physics, 19, 8339-8361,https://doi.org/10.5194/acp-19-8339-2019, 2019.

Lv, Q., Liu, H. B., Wang, J. T., Liu, H., and Shang, Y.: Multiscale analysis on spatiotemporal dynamics of energy consumption CO2 emissions in China: Utilizing the integrated of DMSP-OLS and NPP-VIIRS nighttime light datasets, Science of the Total Environment, 703,https://doi.org/10.1016/j.scitotenv.2019.134394, 2020.

Ma, D., Wang, T., Xu, B., Song, R., Gao, L., Chen, H., Ren, X., Li, S., Zhuang, B., and Li, M.: The mutual interactions among ozone, fine particulate matter, and carbon dioxide on summer monsoon climate in East Asia, Atmospheric Environment, 119668, 2023.

Ma, Z., Xu, J., Quan, W., Zhang, Z., Lin, W., and Xu, X.: Significant increase of surface ozone at

a rural site, north of eastern China, Atmospheric Chemistry and Physics, 16, 3969-3977,https://doi.org/10.5194/acp-16-3969-2016, 2016.

Monks, P. S., Archibald, A. T., Colette, A., Cooper, O., Coyle, M., Derwent, R., Fowler, D., Granier, C., Law, K. S., Mills, G. E., Stevenson, D. S., Tarasova, O., Thouret, V., von Schneidemesser, E., Sommariva, R., Wild, O., and Williams, M. L.: Tropospheric ozone and its precursors from the urban to the global scale from air quality to short-lived climate forcer, Atmos. Chem. Phys., 15, 8889-8973,https://doi.org/10.5194/acp-15-8889-2015, 2015.

Monson, R. K. and Fall, R.: ISOPRENE EMISSION FROM ASPEN LEAVES - INFLUENCE OF ENVIRONMENT AND RELATION TO PHOTOSYNTHESIS AND PHOTORESPIRATION, Plant Physiology, 90, 267-274,https://doi.org/10.1104/pp.90.1.267, 1989.

Mousavinezhad, S., Choi, Y., Pouyaei, A., Ghahremanloo, M., and Nelson, D. L.: A comprehensive investigation of surface ozone pollution in China, 2015-2019: Separating the contributions from meteorology and precursor emissions, Atmospheric Research, 257,https://doi.org/10.1016/j.atmosres.2021.105599, 2021.

Pfister, G. G., Walters, S., Lamarque, J. F., Fast, J., Barth, M. C., Wong, J., Done, J., Holland, G., and Bruyere, C. L.: Projections of future summertime ozone over the US, Journal of Geophysical Research-Atmospheres, 119, 5559-5582,https://doi.org/10.1002/2013jd020932, 2014.

Possell, M., Hewitt, C. N., and Beerling, D. J.: The effects of glacial atmospheric CO2 concentrations and climate on isoprene emissions by vascular plants, Global Change Biology, 11, 60-69,https://doi.org/10.1111/j.1365-2486.2004.00889.x, 2005.

Pu, X., Wang, T. J., Huang, X., Melas, D., Zanis, P., Papanastasiou, D. K., and Poupkou, A.: Enhanced surface ozone during the heat wave of 2013 in Yangtze River Delta region, China, Science of the Total Environment, 603, 807-816,https://doi.org/10.1016/j.scitotenv.2017.03.056, 2017.

Rapparini, F., Baraldi, R., Miglietta, F., and Loreto, F.: Isoprenoid emission in trees of Quercus pubescens and Quercus ilex with lifetime exposure to naturally high CO2 environment, Plant Cell and Environment, 27, 381-391,https://doi.org/10.1111/j.1365-3040.2003.01151.x, 2004.

Ren, S. G., Yuan, B. L., Ma, X., and Chen, X. H.: International trade, FDI (foreign direct investment) and embodied CO2 emissions: A case study of Chinas industrial sectors, China Economic Review, 28, 123-134,https://doi.org/10.1016/j.chieco.2014.01.003, 2014.

Reynolds, R. W., Rayner, N. A., Smith, T. M., Stokes, D. C., and Wang, W. Q.: An improved in situ and satellite SST analysis for climate, Journal of Climate, 15, 1609-1625,https://doi.org/10.1175/1520-0442(2002)015<1609:Aiisas>2.0.Co;2, 2002.

Rosenstiel, T. N., Potosnak, M. J., Griffin, K. L., Fall, R., and Monson, R. K.: Increased CO2 uncouples growth from isoprene emission in an agriforest ecosystem, Nature, 421, 256-259,https://doi.org/10.1038/nature01312, 2003.

Sanchez-Ccoyllo, O. R., Ynoue, R. Y., Martins, L. D., and Andrade, M. d. F.: Impacts of ozone precursor limitation and meteorological variables on ozone concentration in Sao Paulo, Brazil, Atmospheric Environment, 40, S552-S562,https://doi.org/10.1016/j.atmosenv.2006.04.069, 2006.

Schimel, D., Stephens, B. B., and Fisher, J. B.: Effect of increasing CO2 on the terrestrial carbon cycle, Proceedings of the National Academy of Sciences of the United States of America,

112, 436-441,https://doi.org/10.1073/pnas.1407302112, 2015.
Shalaby, A., Zakey, A. S., Tawfik, A. B., Solmon, F., Giorgi, F., Stordal, F., Sillman, S., Zaveri, R. A., and Steiner, A. L.: Implementation and evaluation of online gas-phase chemistry within a regional climate model (RegCM-CHEM4), Geoscientific Model Development, 5, 741-760,https://doi.org/10.5194/gmd-5-741-2012, 2012.
Sharkey, T. D., Loreto, F., and Delwiche, C. F.: HIGH-CARBON DIOXIDE AND SUN SHADE EFFECTS ON ISOPRENE EMISSION FROM OAK AND ASPEN TREE LEAVES, Plant Cell and Environment, 14, 333-338,https://doi.org/10.1111/j.1365-3040.1991.tb01509.x, 1991.
Shen, L., Mickley, L. J., and Gilleland, E.: Impact of increasing heat waves on US ozone episodes in the 2050s: Results from a multimodel analysis using extreme value theory, Geophysical Research Letters, 43, 4017-4025,https://doi.org/10.1002/2016gl068432, 2016.
Shen, L., Jacob, D. J., Liu, X., Huang, G., Li, K., Liao, H., and Wang, T.: An evaluation of the ability of the Ozone Monitoring Instrument (OMI) to observe boundary layer ozone pollution across China: application to 2005-2017 ozone trends, Atmospheric Chemistry and Physics, 19, 6551-6560,https://doi.org/10.5194/acp-19-6551-2019, 2019.
Shen, L., Liu, J., Zhao, T., Xu, X., Han, H., Wang, H., and Shu, Z.: Atmospheric transport drives regional interactions of ozone pollution in China, Science of the Total Environment, 830,https://doi.org/10.1016/j.scitotenv.2022.154634, 2022.
Shetter, R. E., Cinquini, L., Lefer, B. L., Hall, S. R., and Madronich, S.: Comparison of airborne measured and calculated spectral actinic flux and derived photolysis frequencies during the PEM Tropics B mission, Journal of Geophysical Research-Atmospheres, 108,https://doi.org/10.1029/2001jd001320, 2002.
Shi, K. F., Chen, Y., Yu, B. L., Xu, T. B., Chen, Z. Q., Liu, R., Li, L. Y., and Wu, J. P.: Modeling spatiotemporal CO2 (carbon dioxide) emission dynamics in China from DMSP-OLS nighttime stable light data using panel data analysis, Applied Energy, 168, 523-533,https://doi.org/10.1016/j.apenergy.2015.11.055, 2016.
Singh, S. and Singh, R.: High-altitude clear-sky direct solar ultraviolet irradiance at Leh and Hanle in the western Himalayas: Observations and model calculations, Journal of Geophysical Research-Atmospheres, 109,https://doi.org/10.1029/2004jd004854, 2004.
Steiner, A. L., Davis, A. J., Sillman, S., Owen, R. C., Michalak, A. M., and Fiore, A. M.: Observed suppression of ozone formation at extremely high temperatures due to chemical and biophysical feedbacks, Proceedings of the National Academy of Sciences of the United States of America, 107, 19685-19690,https://doi.org/10.1073/pnas.1008336107, 2010.
Sun, Z. H., Hve, K., Vislap, V., and Niinemets, U.: Elevated CO2 magnifies isoprene emissions under heat and improves thermal resistance in hybrid aspen, Journal of Experimental Botany, 64, 5509-5523,https://doi.org/10.1093/jxb/ert318, 2013.
Tai, A. P. K., Mickley, L. J., Heald, C. L., and Wu, S. L.: Effect of CO2 inhibition on biogenic isoprene emission: Implications for air quality under 2000 to 2050 changes in climate, vegetation, and land use, Geophysical Research Letters, 40, 3479-3483,https://doi.org/10.1002/grl.50650, 2013.
Tie, X. X., Madronich, S., Walters, S., Zhang, R. Y., Rasch, P., and Collins, W.: Effect of clouds on photolysis and oxidants in the troposphere, Journal of Geophysical Research-Atmospheres, 108,https://doi.org/10.1029/2003jd003659, 2003.

Verstraeten, W. W., Neu, J. L., Williams, J. E., Bowman, K. W., Worden, J. R., and Boersma, K. F.: Rapid increases in tropospheric ozone production and export from China (vol 8, pg 690, 2015), Nature Geoscience, 9, 643-643,https://doi.org/10.1038/ngeo2768, 2016.

Wang, L. T., Wei, Z., Yang, J., Zhang, Y., Zhang, F. F., Su, J., Meng, C. C., and Zhang, Q.: The 2013 severe haze over southern Hebei, China: model evaluation, source apportionment, and policy implications, Atmospheric Chemistry and Physics, 14, 3151-3173,https://doi.org/10.5194/acp-14-3151-2014, 2014.

Wang, N., Lyu, X. P., Deng, X. J., Huang, X., Jiang, F., and Ding, A. J.: Aggravating O-3 pollution due to NOx emission control in eastern China, Science of the Total Environment, 677, 732-744,https://doi.org/10.1016/j.scitotenv.2019.04.388, 2019a.

Wang, P., Guo, H., Hu, J., Kota, S. H., Ying, Q., and Zhang, H.: Responses of PM2.5 and O-3 concentrations to changes of meteorology and emissions in China, Science of the Total Environment, 662, 297-306,https://doi.org/10.1016/j.scitotenv.2019.01.227, 2019b.

Wang, T., Dai, J., Lam, K. S., Nan Poon, C., and Brasseur, G. P.: Twenty-Five Years of Lower Tropospheric Ozone Observations in Tropical East Asia: The Influence of Emissions and Weather Patterns, Geophysical Research Letters, 46, 11463-11470,https://doi.org/10.1029/2019gl084459, 2019c.

Wang, T., Xue, L., Brimblecombe, P., Lam, Y. F., Li, L., and Zhang, L.: Ozone pollution in China: A review of concentrations, meteorological influences, chemical precursors, and effects, Science of the Total Environment, 575, 1582-1596,https://doi.org/10.1016/j.scitotenv.2016.10.081, 2017a.

Wang, W. N., Cheng, T. H., Gu, X. F., Chen, H., Guo, H., Wang, Y., Bao, F. W., Shi, S. Y., Xu, B. R., Zuo, X., Meng, C., and Zhang, X. C.: Assessing Spatial and Temporal Patterns of Observed Ground-level Ozone in China, Scientific Reports, 7,https://doi.org/10.1038/s41598-017-03929-w, 2017b.

Wang, X., Chen, F., Wu, Z., Zhang, M., Tewari, M., Guenther, A., and Wiedinmyer, C.: Impacts of Weather Conditions Modified by Urban Expansion on Surface Ozone: Comparison between the Pearl River Delta and Yangtze River Delta Regions, Advances in Atmospheric Sciences, 26, 962-972,https://doi.org/10.1007/s00376-009-8001-2, 2009.

Wang, Y., Chen, H., Wu, Q., Chen, X., Wang, H., Gbaguidi, A., Wang, W., and Wang, Z.: Three-year, 5 km resolution China PM2.5 simulation: Model performance evaluation, Atmospheric Research, 207, 1-13,https://doi.org/10.1016/j.atmosres.2018.02.016, 2018.

Wang, Y., Gao, W., Wang, S., Song, T., Gong, Z., Ji, D., Wang, L., Liu, Z., Tang, G., Huo, Y., Tian, S., Li, J., Li, M., Yang, Y., Chu, B., Petaja, T., Kerminen, V.-M., He, H., Hao, J., Kulmala, M., Wang, Y., and Zhang, Y.: Contrasting trends of PM2.5 and surface-ozone concentrations in China from 2013 to 2017, National Science Review, 7, 1331-1339,https://doi.org/10.1093/nsr/nwaa032, 2020.

Wei, J., Li, Z. Q., Li, K., Dickerson, R. R., Pinker, R. T., Wang, J., Liu, X., Sun, L., Xue, W. H., and Cribb, M.: Full-coverage mapping and spatiotemporal variations of ground-level ozone (O3) pollution from 2013 to 2020 across China, Remote Sensing of Environment, 270,https://doi.org/10.1016/j.rse.2021.112775, 2022.

Wilkinson, M. J., Monson, R. K., Trahan, N., Lee, S., Brown, E., Jackson, R. B., Polley, H. W., Fay, P. A., and Fall, R.: Leaf isoprene emission rate as a function of atmospheric CO2 concentration, Global Change Biology, 15, 1189-1200,https://doi.org/10.1111/j.1365-2486.2008.01803.x, 2009.

Wu, W., Xue, W., Lei, Y., and Wang, J.: Sensitivity analysis of ozone in Beijing-Tianjin-Hebei

(BTH) and its surrounding area using OMI satellite remote sensing data, China Environmental Science, 38, 1201-1208, 2018.

Xie, X., Huang, X., Wang, T., Li, M., Li, S., and Chen, P.: Simulation of Non-Homogeneous CO2 and Its Impact on Regional Temperature in East Asia, Journal of Meteorological Research, 32, 456-468,https://doi.org/10.1007/s13351-018-7159-x, 2018.

Xie, X., Wang, T., Yue, X., Li, S., Zhuang, B., and Wang, M.: Effects of atmospheric aerosols on terrestrial carbon fluxes and CO2 concentrations in China, Atmospheric Research, 237,https://doi.org/10.1016/j.atmosres.2020.104859, 2020.

Xie, X., Wang, T., Yue, X., Li, S., Zhuang, B., Wang, M., and Yang, X.: Numerical modeling of ozone damage to plants and its effects on atmospheric CO2 in China, Atmospheric Environment, 217,https://doi.org/10.1016/j.atmosenv.2019.116970, 2019.

Xu, B., Wang, T., Ma, D., Song, R., Zhang, M., Gao, L., Li, S., Zhuang, B., Li, M., and Xie, M.: Impacts of regional emission reduction and global climate change on air quality and temperature to attain carbon neutrality in China, Atmospheric Research, 279,https://doi.org/10.1016/j.atmosres.2022.106384, 2022a.

Xu, B. Y., Wang, T. J., Ma, D. Y., Song, R., Zhang, M., Gao, L. B., Li, S., Zhuang, B. L., Li, M. M., and Xie, M.: Impacts of regional emission reduction and global climate change on air quality and temperature to attain carbon neutrality in China, Atmospheric Research, 279,https://doi.org/10.1016/j.atmosres.2022.106384, 2022b.

Xu, W., Xu, X., Lin, M., Lin, W., Tarasick, D., Tang, J., Ma, J., and Zheng, X.: Long-term trends of surface ozone and its influencing factors at the Mt Waliguan GAW station, China - Part 2: The roles of anthropogenic emissions and climate variability, Atmospheric Chemistry and Physics, 18, 773-798,https://doi.org/10.5194/acp-18-773-2018, 2018.

Yang, Y., Liao, H., and Li, J.: Impacts of the East Asian summer monsoon on interannual variations of summertime surface-layer ozone concentrations over China, Atmospheric Chemistry and Physics, 14, 6867-6879,https://doi.org/10.5194/acp-14-6867-2014, 2014.

Yin, C., Wang, T., Solmon, F., Mallet, M., and Zhuang, B.: Assessment of direct radiative forcing due to secondary organic aerosol over China with a regional climate model, Tellus Series B-chemical & Physical Meteorology, 67,https://doi.org/10.3402/tellusb.v67.24634, 2015.

Yin, Z. and Ma, X.: Meteorological conditions contributed to changes in dominant patterns of summer ozone pollution in Eastern China, Environmental Research Letters, 15,https://doi.org/10.1088/1748-9326/abc915, 2020.

Yoo, J. M., Lee, Y. R., Kim, D., Jeong, M. J., Stockwell, W. R., Kundu, P. K., Oh, S. M., Shin, D. B., and Lee, S. J.: New indices for wet scavenging of air pollutants (O-3, CO, NO2, SO2, and PM10) by summertime rain, Atmospheric Environment, 82, 226-237,https://doi.org/10.1016/j.atmosenv.2013.10.022, 2014.

Yue, X. and Unger, N.: The Yale Interactive terrestrial Biosphere model version 1.0: description, evaluation and implementation into NASA GISS ModelE2, Geoscientific Model Development,https://doi.org/10.5194/gmd-8-2399-2015, 2015.

Zaveri, R. A. and Peters, L. K.: A new lumped structure photochemical mechanism for large-scale applications, Journal of Geophysical Research Atmospheres, 104, 30387-30415,https://doi.org/10.1029/1999JD900876, 1999.

Zhai, S. X., Jacob, D. J., Wang, X., Shen, L., Li, K., Zhang, Y. Z., Gui, K., Zhao, T. L., and Liao, H.: Fine particulate matter (PM2.5) trends in China, 2013-2018: separating contributions from anthropogenic emissions and meteorology, Atmospheric Chemistry and Physics, 19, 11031-11041,https://doi.org/10.5194/acp-19-11031-2019, 2019.

Zhang, H. F., Chen, B. Z., van der Laan-Luijkx, I. T., Chen, J., Xu, G., Yan, J. W., Zhou, L. X., Fukuyama, Y., Tans, P. P., and Peters, W.: Net terrestrial CO2 exchange over China during 2001-2010 estimated with an ensemble data assimilation system for atmospheric CO2, Journal of Geophysical Research-Atmospheres, 119, 3500-3515,https://doi.org/10.1002/2013jd021297, 2014.

Zhao, S., Yu, Y., Yin, D., Qin, D., He, J., and Dong, L.: Spatial patterns and temporal variations of six criteria air pollutants during 2015 to 2017 in the city clusters of Sichuan Basin, China, Science of the Total Environment, 624, 540-557,https://doi.org/10.1016/j.scitotenv.2017.12.172, 2018.

Zheng, B., Tong, D., Li, M., Liu, F., Hong, C., Geng, G., Li, H., Li, X., Peng, L., Qi, J., Yan, L., Zhang, Y., Zhao, H., Zheng, Y., He, K., and Zhang, Q.: Trends in China's anthropogenic emissions since 2010 as the consequence of clean air actions, Atmospheric Chemistry and Physics, 18, 14095-14111,https://doi.org/10.5194/acp-18-14095-2018, 2018.

Zheng, J., Shao, M., Che, W., Zhang, L., Zhong, L., Zhang, Y., and Streets, D.: Speciated VOC Emission Inventory and Spatial Patterns of Ozone Formation Potential in the Pearl River Delta, China, Environmental Science & Technology, 43, 8580-8586,https://doi.org/10.1021/es901688e, 2009.

Zheng, S., Cao, C. X., and Singh, R. P.: Comparison of ground based indices (API and AQI) with satellite based aerosol products, Science of the Total Environment, 488, 400-414,https://doi.org/10.1016/j.scitotenv.2013.12.074, 2014.

Zhuang, B. L., Li, S., Wang, T. J., Liu, J., Chen, H. M., Chen, P. L., Li, M. M., and Xie, M.: Interaction between the Black Carbon Aerosol Warming Effect and East Asian Monsoon Using RegCM4, Journal of Climate, 31, 9367-9388,https://doi.org/10.1175/jcli-d-17-0767.1, 2018.